Salt mobilisation in a floodplain environment: Using EM techniques to identify mechanisms that alter the distribution of saline groundwater

Thesis submitted in accordance with the requirements of the University of Adelaide for an Honours Degree in Geophysics

David Hamilton-Smith

November 2013

THE UNIVERSITY of ADELAIDE

TITLE

Salt mobilisation through natural inundation: Using electromagnetic techniques to identify mechanisms that alter the distribution of saline groundwater.

RUNNING TITLE

Floodplain freshening through lateral flow

ABSTRACT

River Murray floodplain systems have become highly salinised through river regulation and historical irrigation practices. Naturally, floodplain inundation is the hydraulic mechanism that reduces the concentration of salt on the floodplain. Flushing of saline groundwater through lateral flow following river recession post flooding was previously unidentified. Geophysical techniques have been utilised to collect subsurface conductivity data on Clark's Floodplain, a typical Murray floodplain system. Conductivity data on the floodplain is well constrained, and change in its distribution after the 2010/2011 River Murray flood has been interpreted to identify three freshening mechanisms. They include vertical infiltration of flood water and bank recharge during overbank flows, as well as lateral flow of groundwater after river regression.

KEYWORDS

Salinity, flooding, inundation, freshening, groundwater, lateral flow, TEM

TABLE OF CONTENTS

LIST OF FIGURES AND TABLES

INTRODUCTION

The health of the River Murray and its associated floodplains has been under threat due to increased salinity brought on by unnatural river regulation and improper irrigation practices. The environmental health of floodplain biota is majorly governed by natural inundation events which negate the impact of pervasive saline aquifers that underlie large parts of the Murray Darling Basin (Bren 1992). The duration, timing and magnitude of flooding has been altered through intense river regulation and usage for agricultural practices.

Due to high variability of river flow in arid and semi-arid regions, manipulation of river systems through the installation of weirs and storage infrastructure has become a common practice (Jolly et al. 1998). Interaction of surface and groundwater in floodplain wetlands is affected by river regulation through water table elevation and associated increased salt accumulation rates in floodplain soils (Jolly et al. 1993). A reduction in the duration, timing and magnitude of inundation reduces the flushing of salt within the vadose and elevated phreatic zones, reducing soil water availability for floodplain vegetation (Jolly et al. 2008).

Groundwater mounds have formed below the highlands adjacent to floodplains in response to irrigation in agricultural regions (Holland et al. 2013). These hydrogeological features create a hydraulic gradient from regional saline aquifers to adjoining floodplains. In the lower River Murray, the inflow of saline groundwater has increased by a factor of 3 since development for agricultural use, attributing to elevated salinisation is floodplain aquifers (Holland et al. 2013).

On the South Australian portion of the River Murray, floodplain salinisation from irregular flooding has been a broadly researched topic, particularly within the Bookpurnong region (Berens et al. 2009a, Berens et al. 2009b, White et al. 2009, Munday et al. 2007). The Living Murray initiative was founded in response to the evidence supporting the decline of the River Murray and its floodplain condition. A number of water management trials were employed to test strategies to improve the health of Clark's Floodplain by reducing the presence of saline groundwater in the near-surface region (Berens et al. 2009a). For example, Artificial inundation was trialled with promising results, however it was noted that this was not a long term solution, and natural flooding events would be necessary to restore floodplain health (White et al. 2009).

An active groundwater management solution was incorporated on Clark's Floodplain in the form of a Salt Interception Scheme (SIS). Infrastructure was installed along the base of the highland in 2005. SIS utilise large-scale groundwater pumping bores to intercept natural, irrigation and river regulation induced groundwater flows (Forward 2004). Similarly, the Living Murray Pumping Bore (LMPB) was installed to in 2006 to withdraw saline groundwater near the river, to encourage bank recharge in a localised area (Berens et al. 2009a).

Electromagnetic (EM) techniques measure sub-surface conductivity and have been used in the Bookpurnong region to map conductivity data. These surveys have been run to estimate the distribution of saline groundwater within the floodplain system. Changes in

this distribution have been used to measure the effectiveness of salt interception, water management trials and other salt mobilisation methods.

Helicopter electromagnetic (HEM) data were initially acquired in 2005 (Munday et al. 2005, Munday et al. 2007) to aid in the development of a hydrogeologic framework for building SIS boreholes in the Loxton Sands aquifer. Further HEM data were obtained in 2009 (Berens et al. 2009a) to map floodplain and groundwater salinity changes before and after the installation of the Bookpurnong SIS. Data from ground based EM surveys were also utilised by Berens et al. (2009a) and White et al. (2009) to provide information about conductivity changes during a range of floodplain groundwater management trials, including artificial inundation of the floodplain and groundwater interception by the LMPB. These include terrain conductivity meter surveys in 2006 and 2008 and five shallow time domain electromagnetic (TEM) surveys from 2005 to 2011.

Tan et al. (2007) analysed TEM data against the pore fluid salinity of sub-surface sediments. He concluded that, for the 32 validation sites investigated along a stretch of river upstream of this test area, the geophysically determined conductivities strongly correlated with the conductivity of the groundwater in that area.

Salt mobilisation through the lateral flow of highly saline groundwater following natural inundation has not previously been investigated. Overbank flows and floodplain inundation occurred in 2010/2011 in response to high rainfall in the Murray Darling catchment area. This provided a base to further work by gaining a better understanding

of the floodplain inundation process and its effect on groundwater salinity. If it is possible to see changes in geophysical data sets collected after these flooding events, this will suggest an increase or reduction in floodplain salinity facilitated by 1) vertical infiltration from the surface, 2) bank recharge and/or 3) lateral flow of saline groundwater.

In order to identify change in the salinity distribution on the field site, historical conductivity data has been analysed against post-flood conductivity data. To compare historic and post-flood data, acquisition techniques and methods have been kept consistent. A TEM system was used for static and towed acquisition to collectively analyse the vertical and lateral extent of freshening. Terrain conductivity meters were used to collect high horizontal resolution data to determine the near surface conductivity of the vadose zone and top of the water table. A groundwater sonde provided groundwater conductivity data to analyse the extent of freshening through bank recharge and vertical infiltration.

BACKGROUND

Hydrogeology

Clark's Floodplain at Bookpurnong is located in the extensive Murray Basin, as shown in Figure 1. It is an intracratonic basin that formed as a consequence of Australia rifting from Antarctica during the early Cretaceous, and is bound by the Mount Lofty Ranges to the West and the Great Dividing Range to the East (Brown and Stephenson 1991). It is comprised of Cainozoic, flat lying sediments with a maximum thickness of 600m, covering an area of approximately 300,000km² (Brown 1989). On average the

distribution of sediments reaches a depth of 200m, preserving three major quaternary depositional sequences, separated by disconformities (Brown 1989). Sedimentary rocks in the east are weakly lithified, sand, silt and clay, while sedimentary rocks in the central and south-western areas are dominantly marine in nature (Brown and Stephenson 1991).

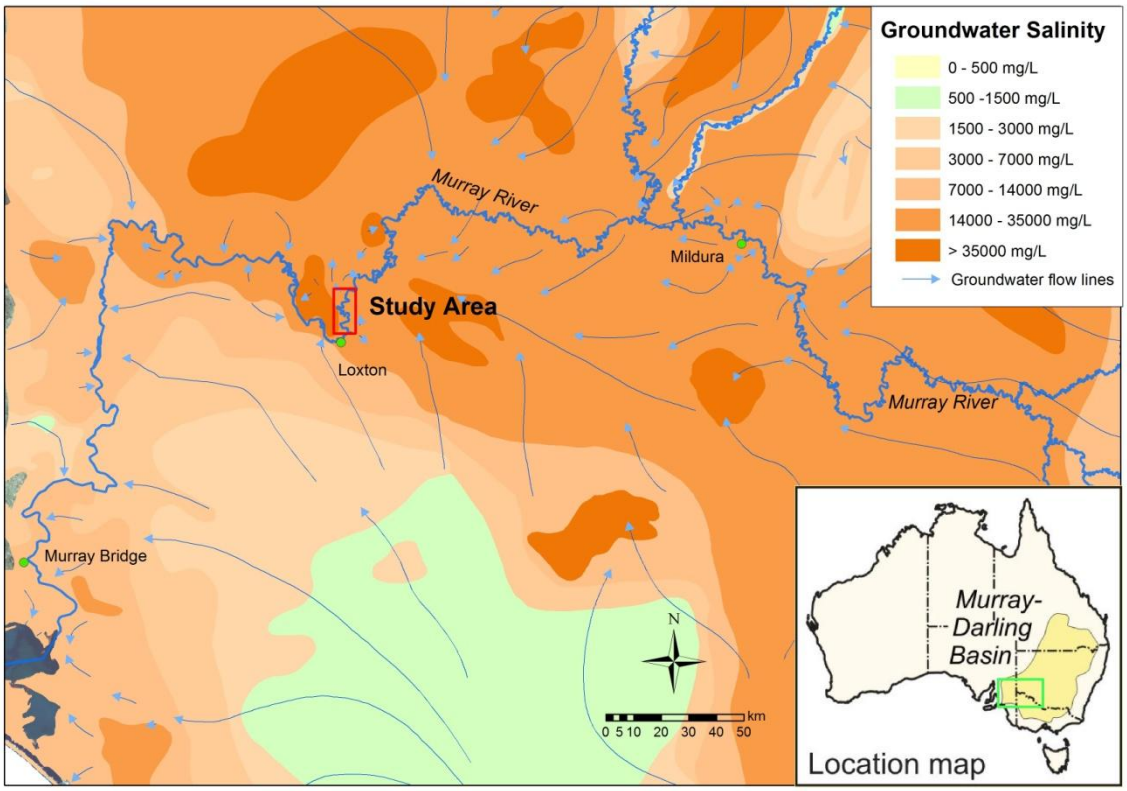

Figure 1: Groundwater salinity of the Lower Murray Basin, South Australia. The location of the study area is indicated with a red polygon. Flow lines indicate the movement of regional groundwater is directed towards the river. Modified from (Hatch et al. 2010).

Tertiary sediments beneath the highland contain saline groundwater which flows into floodplain systems and further into the Murray (Brown 1989). Aquifers initially contained fresh water; however the source of regional groundwater salt is still a contentious topic. Dahlhaus et al. (2000) concluded that salinisation in the western regions of the Murray Basin was caused by dissolution of salt that had accumulated in the regolith during marine intrusions throughout the Miocene and Pliocene. Acworth and Jankowski (2001) and Summerell et al. (2000) concluded that Aeolian processes

produced parna deposits in the eastern zone of the basin, containing dust, and salt likely derived from Central Australia. Brown (1989) and Cartwright et al. (2004) argue that salinity increased through evapotranspiration in areas where groundwater has risen to the capillary zone during semi-arid to arid climatic conditions. This process is still observed today and has caused the near-surface aquifers, such as those of interest in this study, to be highly salinised (Brown 1989).

The two geological units of primary interest to this project situated on the floodplain are the near-surface Coonambidgal Clay and Monoman formations (Brown and Stephenson 1991, Telfer et al. 2004a) (Figure 2). The Coonambidgal was deposited in a low energy fluvial system and consists of upwardly fining sands and clay (Hatch et al. 2010). It acts as an aquitard to the underlying Monoman formation, and thins towards the river (Telfer et al. 2004b).

Groundwater within the floodplain system is contained within the Late Pleistocene to Holocene Monoman Formation, shown in Figure 2 (Brown and Stephenson 1991). The Monoman was deposited in a high energy fluvial environment and is in direct contact with the Murray for most of its extent (Hatch et al. 2010). It consists of fine to coarse silty sands and gravels which infill the incised River Murray valley (Telfer et al. 2004b). High transmissivity is facilitated by its geology and associated porosity and permeability, it is an aquifer of moderate to high hydraulic conductivity (Telfer et al. 2004b). Both floodplain units are terrigenous in nature, products of erosion, transport and reworking driven by the river and deposited on the floodplain (Brown 1989).

In the highland, adjacent to the floodplain three units are important: the Woorinen Sands, the Blanchetown Clay and the Upper Loxton-Parilla Sands (Hatch et al. 2010). The Woorinen Sands are Aeolian in nature, and overlie the low-energy lacustrine Blanchetown Clay (Telfer et al. 2012). The Blanchetown clay acts as a regional aquitard, influencing the rate of vertical infiltration from rainfall and watering (Hatch et al. 2010). The Loxton-Parilla Sands are dominated by medium to coarse sands which act as a regional aquifer (Lewis et al. 2008). Although this unit does not come in direct contact with the floodplain, groundwater flows from the unit into the Monoman Sands aquifer (Lewis et al. 2008, Berens et al. 2009b).

Hydrology

In an arid river system, such as the Murray Basin, discharge of saline water into the floodplain sediments and to the river is primarily regulated by the 'gaining' and 'losing' conditions on the floodplain (Fetter 2001, Lamontagne et al. 2005). Telfer et al. (2012) states that salt accumulation and distribution on the floodplain relates to groundwater level, river level and the rate of evapotranspiration on the floodplain. Groundwater freshening following overbank flows can be facilitated by vertical infiltration and bank recharge during flooding, as well as lateral flow following river recession (Holland et al. 2013, Telfer et al. 2012). A schematic representation of the hydrogeology of the study area is illustrated in Figure 2.

For a floodplain to accumulate salt it must be characterised as a 'gaining floodplain', where the regional groundwater system is discharging into the floodplain alluvium (Telfer et al. 2012). As indicated in Figure 2, the floodplain is often gaining over much of the lower Murray River, as regional water tables are typically elevated above both

river and floodplain level (Telfer et al. 2005). However, net evapotranspiration is often higher than net groundwater flow, preventing the river from gaining groundwater, concentrating salt in the floodplain (Telfer et al. 2004a). If vegetation on the floodplain system is extensive, and evapotranspiration is increased by warm climate, the process will induce the river to lose water to the floodplain, even when the groundwater level is above the river level (Telfer et al. 2004a). Lateral flow from regional groundwater aquifers into the floodplain and river systems is typically saline in the South Australian reaches of the Murray (Rolls 2007).

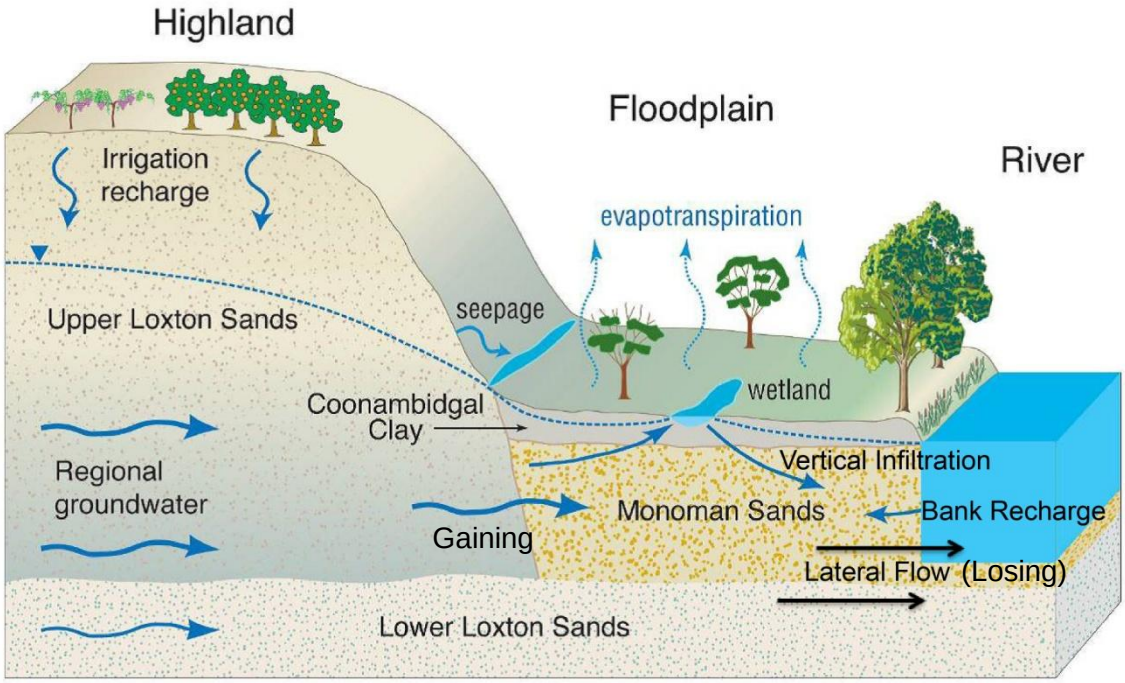

Figure 2: Conceptual model of surface water-groundwater interactions in lower River Murray floodplain wetlands illustrating the location of important groundwater discharge pathways in the floodplain. Adapted from (Holland et al. 2013).

The process in which highly saline groundwater discharges from the floodplain alluvial sediments into the river reach is characterised as a losing floodplain. Losing conditions are facilitated by lateral/base flow and are common along the Murray, due to groundwater levels typically being above the river level (Hatch et al. 2010). It is likely for this process to occur post-inundation of a floodplain, at which time the river level

would have subsided below the elevated water table, creating a hydraulic gradient and encouraging the floodplain to lose saline groundwater to the river, as shown in Figure 2.

During overbank flows, river level is elevated above the floodplain water table, creating a hydraulic gradient moving low salinity river water into the river banks and floodplain alluvium (Holland et al. 2009). This process is known as bank recharge, and forms a lens of fresh river water over comparatively saline groundwater (Doody et al. 2009). In addition, vertical infiltration from the surface reduces both soil chloride concentration, and partly attributes to groundwater freshening (Holland et al. 2013). Water flux of both processes is controlled by the porosity and permeability of the facies being infiltrated.

Flow of saline groundwater into Clark's Floodplain has changed over the past century due to extensive irrigation in the Bookpurnong irrigation district, causing the local water table to rise within the Loxton Sands (REM-Aquateram. 2005). Similarly, clearing of native vegetation, widespread since the development of the River Murray's farming district, has caused the water table to rise, further increasing the hydraulic gradient towards floodplain systems (Dahlhaus et al. 2000).

GEOPHYSICAL METHODS AND ACQUISITION

TEM systems, terrain conductivity meters and a groundwater sonde were utilised to collect conductivity data on Clark's Floodplain. Static TEM provided analysis of the floodplain aquifer system at depth, while towed TEM improved the distribution of data, due to its fast sampling rate and broad spatial range. "Geonics EM31" and "GF Instruments CMD-4" terrain conductivity meters were used to produce information of the conductivity distribution within the top 6m of the floodplain. Four bore holes were

logged using a "YSI XLM600 sonde", allowing the acquisition of high vertical resolution conductivity data of the floodplain groundwater system. All surveying processes were kept consistent with past data collection, in order to accurately characterise change within the floodplain.

Static and Towed TEM Method

TEM is an inductive electromagnetic technique that acquires conductivity data by recording the decay of an induced magnetic field. Static and moving TEM acquisition methods were utilised for this survey, as they provide high resolution data both vertically and laterally. "Zonge Engineering's NanoTEM" system was used to collect all TEM data for this study.

The transmitter emits a constant current through the loop, inducing a primary magnetic field. A very quick turn off occurs (approximately 1.5μs), inducing a current into the conductive ground. This current produces a secondary magnetic field which decays due to the attenuation of current from resistance in the ground and induced eddy currents. This field is vertical in the middle of the receiving loop, producing a second electromotive force which is then recorded as a voltage decay. The signal is recorded in decay-time windows which are arranged as logarithmically increasing functions to improve the signal/noise ratio (Fitterman and Stewart 1986).

For the towed TEM, a single turn 3m x 3m transmitter and a 1m x 1m receiver was used for trial purposes (Figure 3). Additionally a triple turn configuration was also used in order to remain consistent with past TEM surveys. The antennas were towed at

approximately 6km/h. Five vehicular tracks on the floodplain covered approximately 4km (survey locations depicted in towed TEM plots).

Static TEM soundings were made using a static, single turn 20m x 20m transmitting loop and a single turn 5m x 5m receiver loop, providing a penetration depth of 50-80m. A 500m transect was covered by 25 consecutive stations, beginning at the river bank and ending in the central zone of the floodplain (Figure 4).

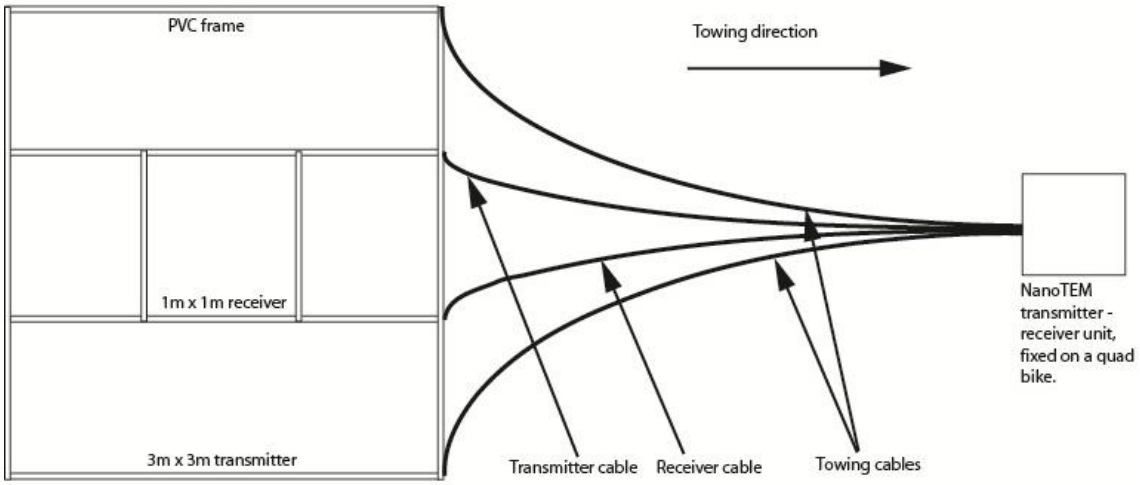

Figure 3: Schematic diagram of the towed TEM rig, modified from(Hatch et al. 2010)

Following acquisition, the TEM data sets were inverted using Zonge Engineering's STEMINV program – a 1D smooth-model layered-earth inversion (Reid et al. 2010). The 1D model is assumed to be valid in subhorizontal, layered sedimentary settings, like those encountered in the study area. Results may be affected by 2D or 3D structures that could cause changes in the sub-surface topography; however these are not common on the study area (Hatch et al. 2010).

Terrain Conductivity Meter

The terrain conductivity meter is an inductive frequency domain electromagnetic (FDEM) technique that records a single conductivity at a specific frequency. A "GF instruments CMD-4" terrain conductivity meter was used to map the response of the near-surface subsurface features within the survey area. Already existing data sets were also analysed, these data sets were collected using a "Geonics EM-31" instrument.

The internal transmitter transmits a sinusoidal current into the ground that induces a primary magnetic field perpendicular to the orientation of the transmitter coil. Eddy currents are produced by the oscillating primary magnetic field in its surroundings. A secondary magnetic field is induced by these currents, and it is dependent on the subsurface conductivity distribution. The internal receiver coil measures the secondary magnetic field, as well as the primary magnetic field. The ratio of the fields can be used to infer the grounds bulk conductivity between approximately 2-6m based on LIN approximation (McNeill 1980a).

Data were collected using a horizontal coplanar dipole configuration, maximising imaging depth. Acquisition occurred on a 50m grid. Data were collected every second, at nominal in-line spacing of approximately 1-2m. Apparent conductivities were LIN corrected, due to the highly conductive characteristics of the floodplain.

Groundwater Conductivity Sonde

Ground conductivity sonding is a galvanic technique that operates on the same principle as a standard water conductivity meter. A fixed spacing dipole-dipole electrode array is used, one dipole is current driven and the other is used to measure the voltage drop (YSI

Sonde User Manual 2011). The measured voltage drop is then converted into a conductance value (YSI Sonde User Manual 2011). A "YSI Multiparameter 600XL" sonde was used to log conductivity in 11 bore holes. Water pressure was measured by a barometer which was translated to water depth.

RESULTS

In this section I will be presenting data collected using three different techniques. These were acquired using a TEM system (both static and moving data will be presented), a terrain conductivity meter and a groundwater sonde, as described in the methods section. Data shown here concentrated on Transect B3, shown in Figure 4. In addition, the location of the LMPB and SIS bores are presented. Table 1 presents all data sets analysed for this study.

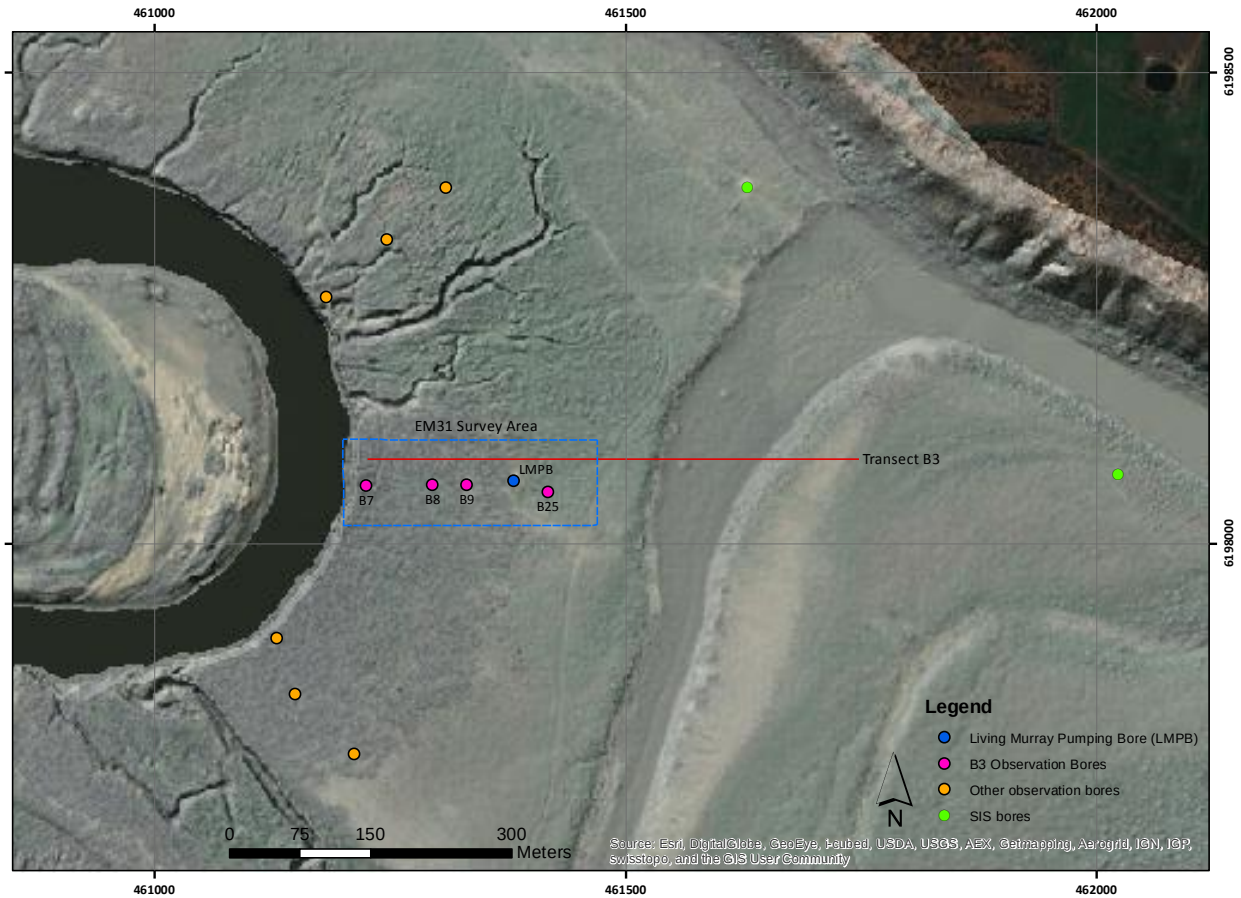

Figure 4: Air photo image and overlayed LiDAR elevation model of the field area. The location of survey zones, transects and observation and pumping well locations displayed.

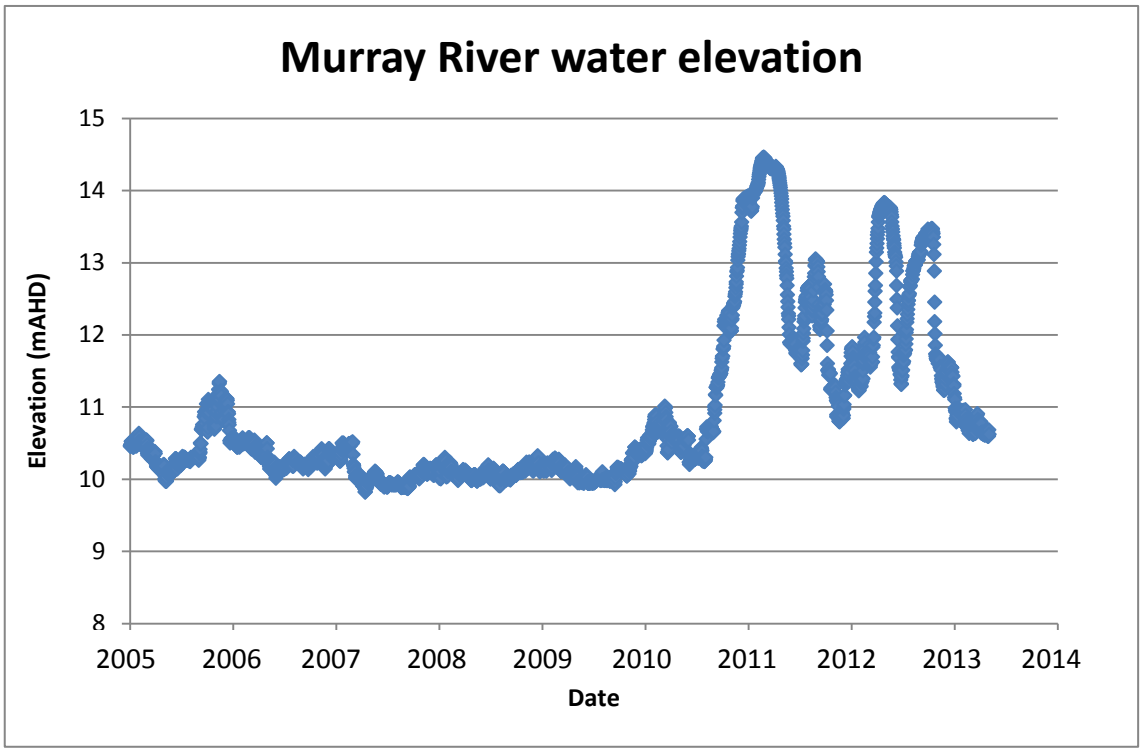

Figure 5: River Murray water elevation data for the period of geophysical surveying on Clark's Floodplain. Data was recorded downstream from Lock 4, approximately 1km north of Clark's Floodplain. Elevation is represented by Australian Height Datum. Produced from Water Connect (2013).

Data have been collected under a variety of climatic conditions. In order to determine the climate in which data was collected, river level data has been presented in Figure 5. Low river level corresponds to times of drought, and high river level corresponds to overbank flow conditions. These data were collected at the Lock 4 gauging station, approximately 1km upstream of the survey site (Water Connect 2013). It is close enough that it is assumed to be consistent with river levels adjacent to Clark's Floodplain. River level from mid-2006 to late 2009 correlated to drought conditions in this part of South Australia. 2008 was the driest period during water management trials and associated geophysical surveying; this corresponds to the peak of the drought. Early 2010 saw a rapid rise in the water level, peaking in March 2011. Clark's Floodplain was inundated throughout this period. The river has receded to approximately 10.5mAHD, close to equilibrium with the water table.

Table 1: Geophysical and groundwater conductivity data collected on Clark's Floodplain from 2005 to 2013.

DATA TYPE	ACQUISITION DATE	ACQUISITION METHOD	ACQUISITION LOCATION
TEM	November 2005	Static in loop	Transect B3
	July 2006	Three turn, towed in loop	Clark's Floodplain vehicular tracks (inc B3)
	November 2007	Static in loop	Transect B3
	December 2008	Three turn, towed out of loop	Clark's Floodplain vehicular tracks (inc. B3)
		Static in loop	Transect B3
	December 2011	Three turn, towed in loop	Clark's Floodplain vehicular tracks (inc. B3)
		Single turn, towed in loop	Clark's Floodplain vehicular tracks (inc. B3)
		Static in loop	Transect B3
	July 2013	Three turn, towed in loop	Clark's Floodplain vehicular tracks (inc. B3)
		Single turn, towed in loop	Clark's Floodplain vehicular tracks (inc. B3)
		Static in loop	Transect B3
SHALLOW TERRAIN CONDUCTIVITY	September 2006	EM31	Transect B3 and close surroundings
	March 2008	EM31	Transect B3 and close surroundings
	July 2013	CMD-4	Transect B3 and close surroundings
GROUNDWATER CONDUCTIVITY	January 2006	Sonde	Observation bores parallel with B3
	July 2006	Sonde	Observation bores parallel with B3
	August 2006	Sonde	Observation bores parallel with B3
	October 2006	Sonde	Observation bores parallel with B3
	November 2006	Sonde	Observation bores parallel with B3
	December 2006	Sonde	Observation bores parallel with B3
	January 2007	Sonde	Observation bores parallel with B3
	March 2007	Sonde	Observation bores parallel with B3
	April 2007	Sonde	Observation bores parallel with B3
	July 2007	Sonde	Observation bores parallel with B3
	February 2008	Sonde	Observation bores parallel with B3
	March 2008	Sonde	Observation bores parallel with B3
	December 2011	Sonde	Observation bores parallel with B3
	July 2013	Sonde	Observation bores parallel with B3

TEM Data

Moving TEM depth-slices and static TEM vertical cross-sections are chronologically ordered from 2005 to 2013, as shown in Figures 6 to 16. All TEM results shown here use a logarithmic colour scale, as the range of conductivities was large. Depth sections are vertically exaggerated, to help determine vertical variability. Where possible, towed

and static TEM are presented together, allowing interpretation of both the near surface and at depth. White zones in the conductivity sections indicate areas where conductivity is less than the indicated limit.

TEM SURVEY 2005

In 2005 static baseline data were acquired to characterise sub-surface conductivity distribution prior to the commencement of water salinity management trials, shown in Figure 6.

Static TEM data from 2005 contain approximately 300 data points that were inverted to produce a 2D three layered sub-surface model (Figure 6). The inverted conductivity model characterises the conductivity distribution of Clark's Floodplain before any of the Living Murray Program infrastructure was built on Clark's Floodplain. A small freshwater lens is evident at the river bank in the top few meters of the floodplain. The remainder of the line is highly conductive, indicating a slight increase in resistivity below 25m depth.

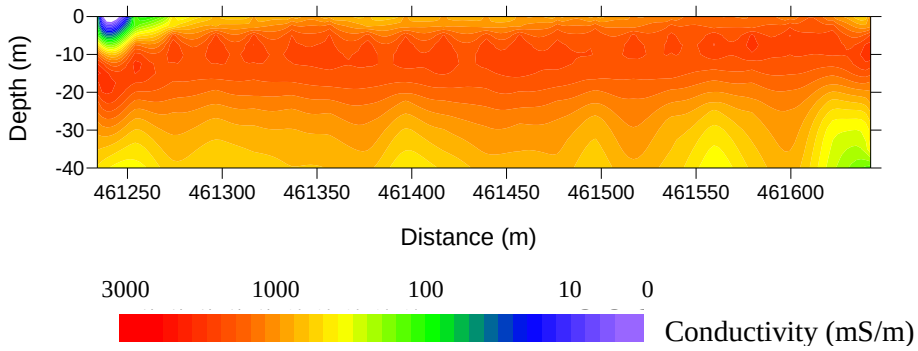

Figure 6: Static TEM vertical cross-section of inverted conductivity data collected in November 2005. The profile is given by transect B3 in Figure 4.

TEM SURVEY 2006

Data collected in July 2006 was part of a larger towed TEM survey that concentrated mostly on an area to the South East of our field site. Only data of interest to this study are shown in Figure 7.

Towed TEM data from 2006 contain approximately 35000 data points that were inverted to produce 2D depth-sliced sub-surface models (Figure 7). Interpretation of inverted data in Figure 7 suggests subsurface conductivity remains relatively uniform

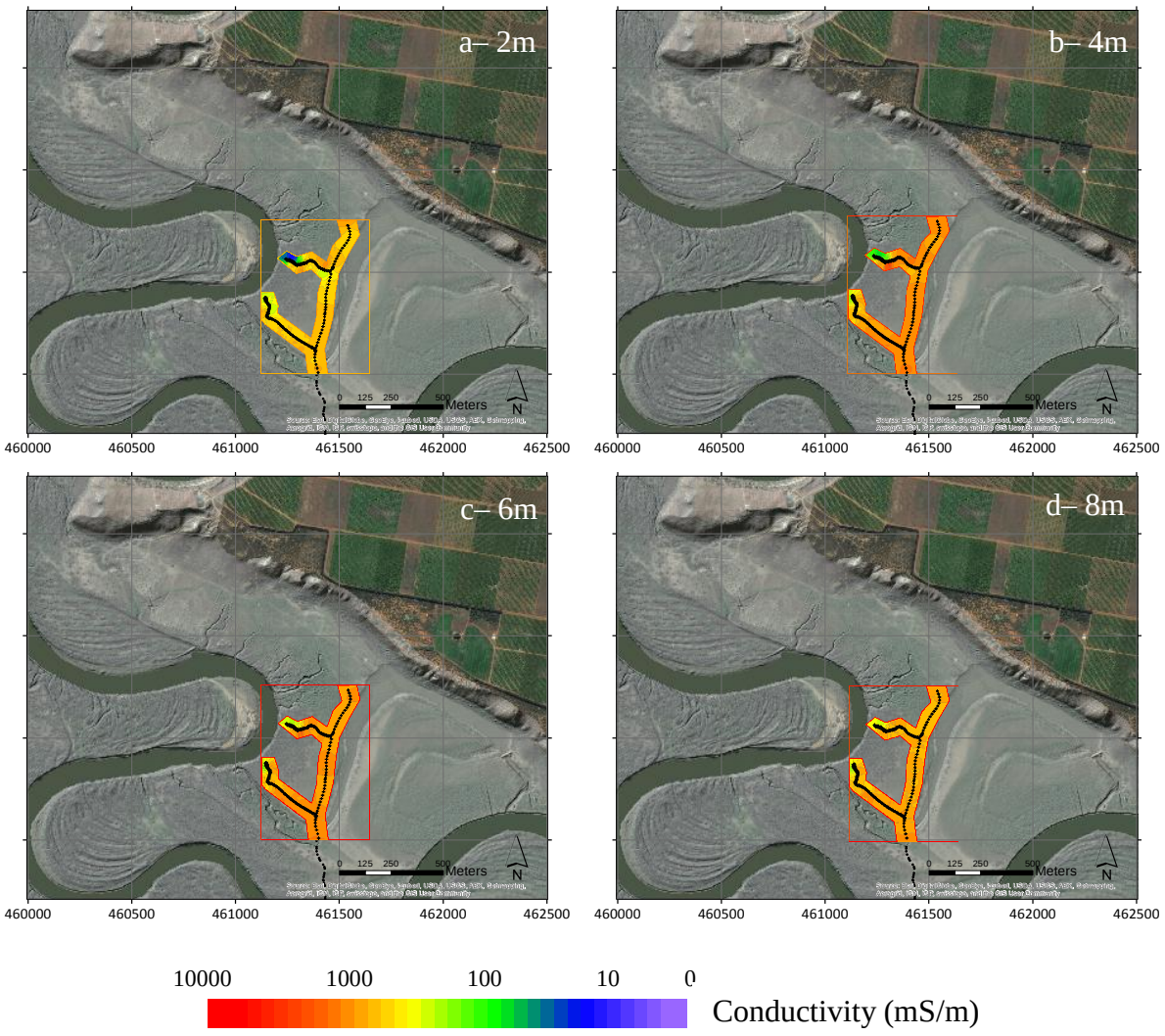

Figure 7: Inverted TEM depth models, a)-d) map views of the conductivity model for 2, 4, 6 and 8m. Data were collected in July 2006 using a triple turn antenna configuration during the drought, in order to characterise the conductivity (salinity) distribution. Survey locations are represented by black markers. See Figure 4 for base-map information.

between 2-8 m, with a majority of groundwater falling in the 1000 mS/m range at all depths. A shallow, less conductive fresh zone exists on the western end of line B3, prevalent between 0-4m. Slight relief associated with this resistor is evident down to 8m. These data were also collected before any of the Living Murray Program infrastructure was built on Clark's Floodplain.

TEM SURVEY 2007

Commencement of the Living Murray pumping occurred in August 2006, ceasing, along with the associated SIS in November 2006. They were both recommissioned in May 2007. Figure 8 shows a line of static TEM collected in November 2007. These data were originally collected to characterise the effectiveness of Living Murray pumping.

Static TEM data from 2007 contain approximately 300 data points that were inverted to produce a 2D three layered sub-surface model (Figure 8). Interpretation of inverted data in Figure 8 suggests an increase in the distribution of the freshwater lens since 2005 (Figure 6), as it migrates eastward. Consequently, the underlying conductive saline groundwater band has been influenced downward with the infringing freshwater lens.

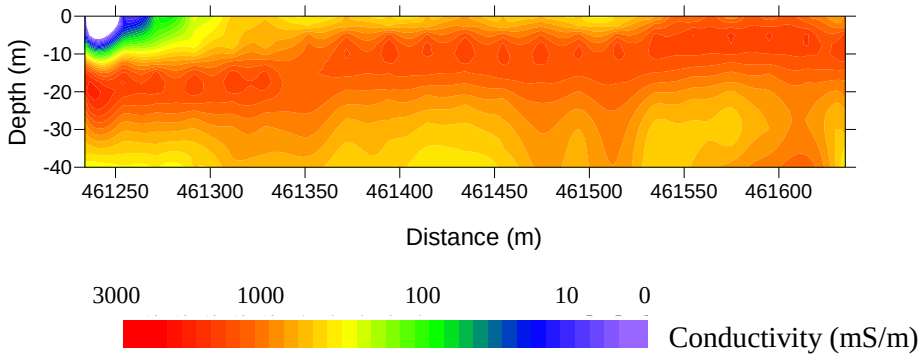

Figure 8: Static TEM vertical cross-section of inverted conductivity data collected in November 2007. The profile is given by transect B3 in Figure 4.

TEM SURVEY 2008

Moving and static TEM data were acquired in December 2008 to characterise the effectiveness of Living Murray (LM) pumping, as well as analysing the conductivity of the remaining floodplain. They are represented in Figures 9 and 10 respectively. It is important to note that the moving TEM data set was collected using an out of loop configuration. It is likely that the resistive zones observed in Figure 9 are inaccurate and may not be as resistive as shown (Hatch, personal comm.).

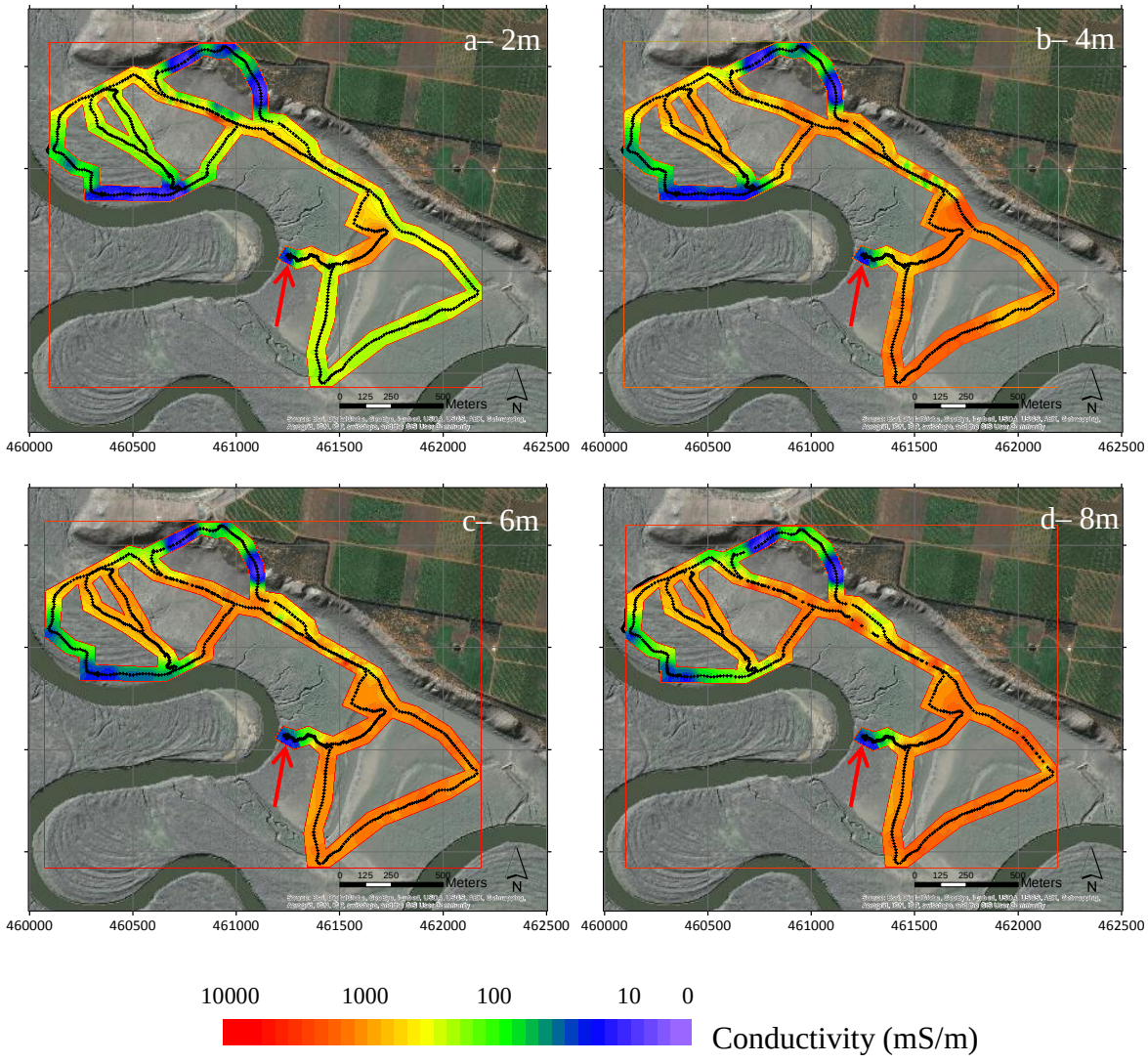

Figure 9: Inverted TEM depth models, a)-d) map views of the conductivity model for 2, 4, 6, and 8m. Data were collected in December 2008 using an out-of-loop triple turn configuration, approximately two years after the installation of the Living Murray pumping bore (LMPB). Survey locations are represented by black markers. Red arrows indicate the highly resistive zone at the end of Transect B3. See Figure 4 for base-map information.

Towed TEM data from 2008 contain approximately 70000 data points that were inverted to produce 2D depth-sliced sub-surface models (Figure 9). As discussed above, the data were collected using an out-of-loop configuration, therefore it is unlikely that the large increase of lateral and vertical extent of the resistive response at the western end of line B3 (highlighted with an arrow on Figure 9) extended to 8m, however some increase is likely. As the LMPB, located near the centre of this line (see Figure 4) had been pumping saline groundwater away from this area since May 2007, it is thought that the increase in resistivity is a collaboration of this response and the out-of-loop configuration.

Static TEM data from 2008 contain approximately 300 data points that were inverted to produce a 2D three layered sub-surface model (Figure 10). Influence of the LMPB is evident, with the freshwater lens migrating further east into the floodplain since 2007 (Figure 8). The distribution of saline groundwater appears to increase with depth, as conductivity has increased below 20m. Conductivity in the top layer of the profile has slightly decreased behind the LMPB (seen in Figure 4) to approximately 461550m

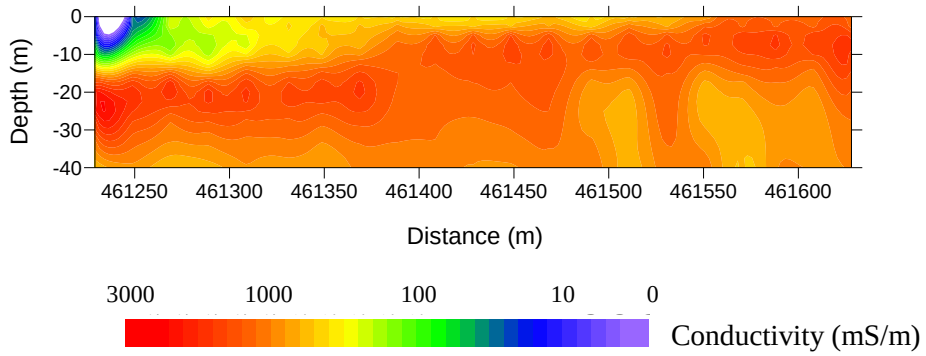

Figure 10: Static TEM vertical cross-section of inverted conductivity data collected in December 2008. The profile is given by transect B3 in Figure 4.

TEM survey 2011

Three data sets were collected in December 2011, each aiming at determining the conductivity distribution after overbank flows on the floodplain. These data were collected approximately 9 months after the major flooding event that affected the river in this area in 2011. Figure 11 shows the triple turn towed TEM, Figure 12 shows a single turn TEM trial and Figure 13 shows the static B3 transect. Note that LM pumping (see Figure 4 for location) stopped in November 2010, over a year prior to the collection of these data sets.

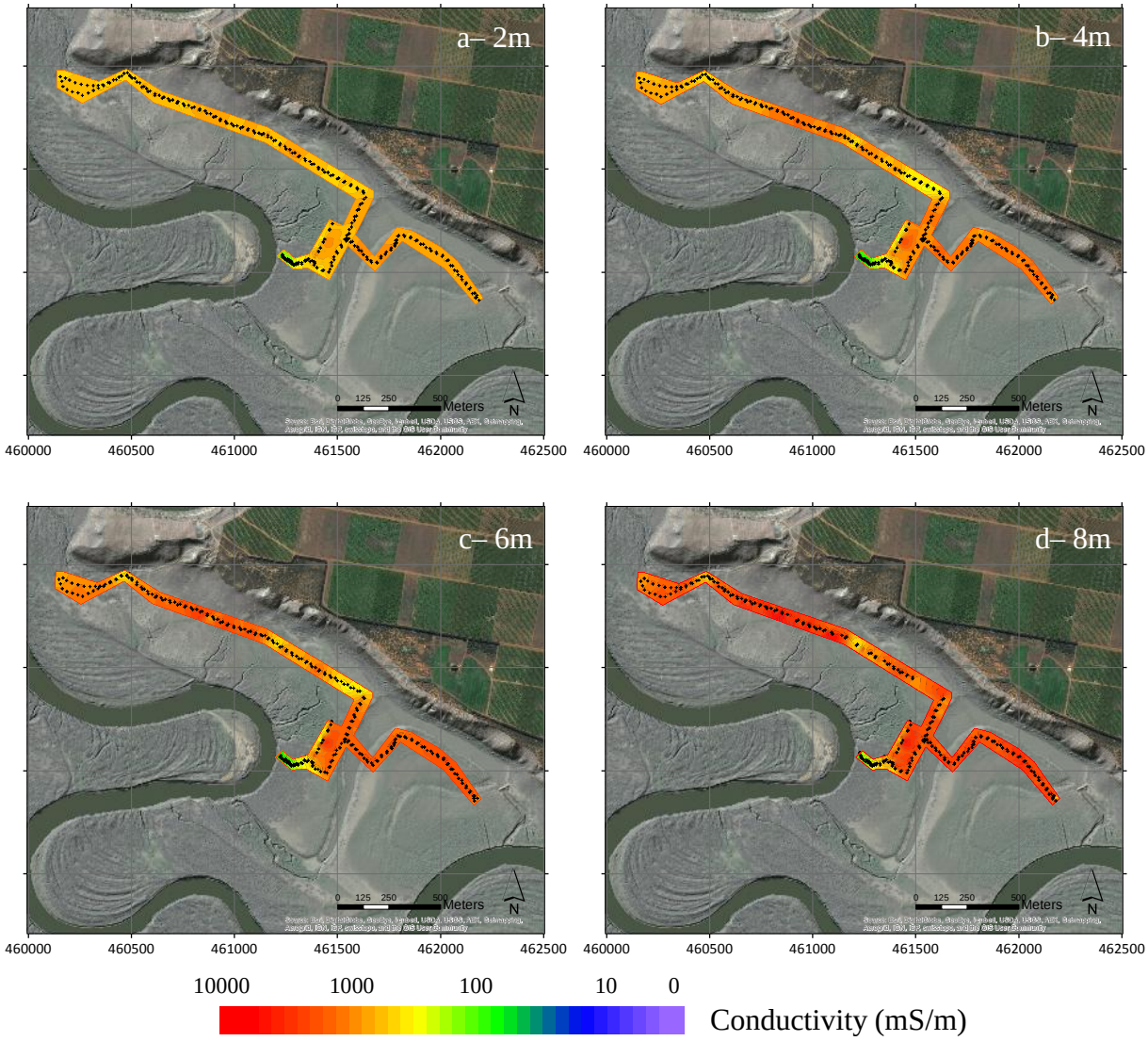

Figure 11: Inverted TEM depth models, a)-d) map views of the conductivity model for 2, 4, 6, and 8m. Data were collected in December 2011 using a triple turn antenna configuration, nine months after the height of the 2010/2011 flood, to characterise the change in conductivity distribution. Survey locations are represented by black markers. See Figure 4 for base-map information.

Triple-turn towed TEM data from 2011 contain approximately 25000 data points that were inverted to produce 2D depth-sliced sub-surface models (Figure 11). The resistive zone at the western end of B3 (see Figure 4) is consistent down to 8m, falling in the 100mS/m range. Conductivity increases with depth in the remainder of the field site. At 2m, conductivities are on the scale of one magnitude more resistive compared to the 8m depth slice (1000mS/m to 10000mS/m). Near-surface freshening is expected after flooding, from saturation of low salinity flood water.

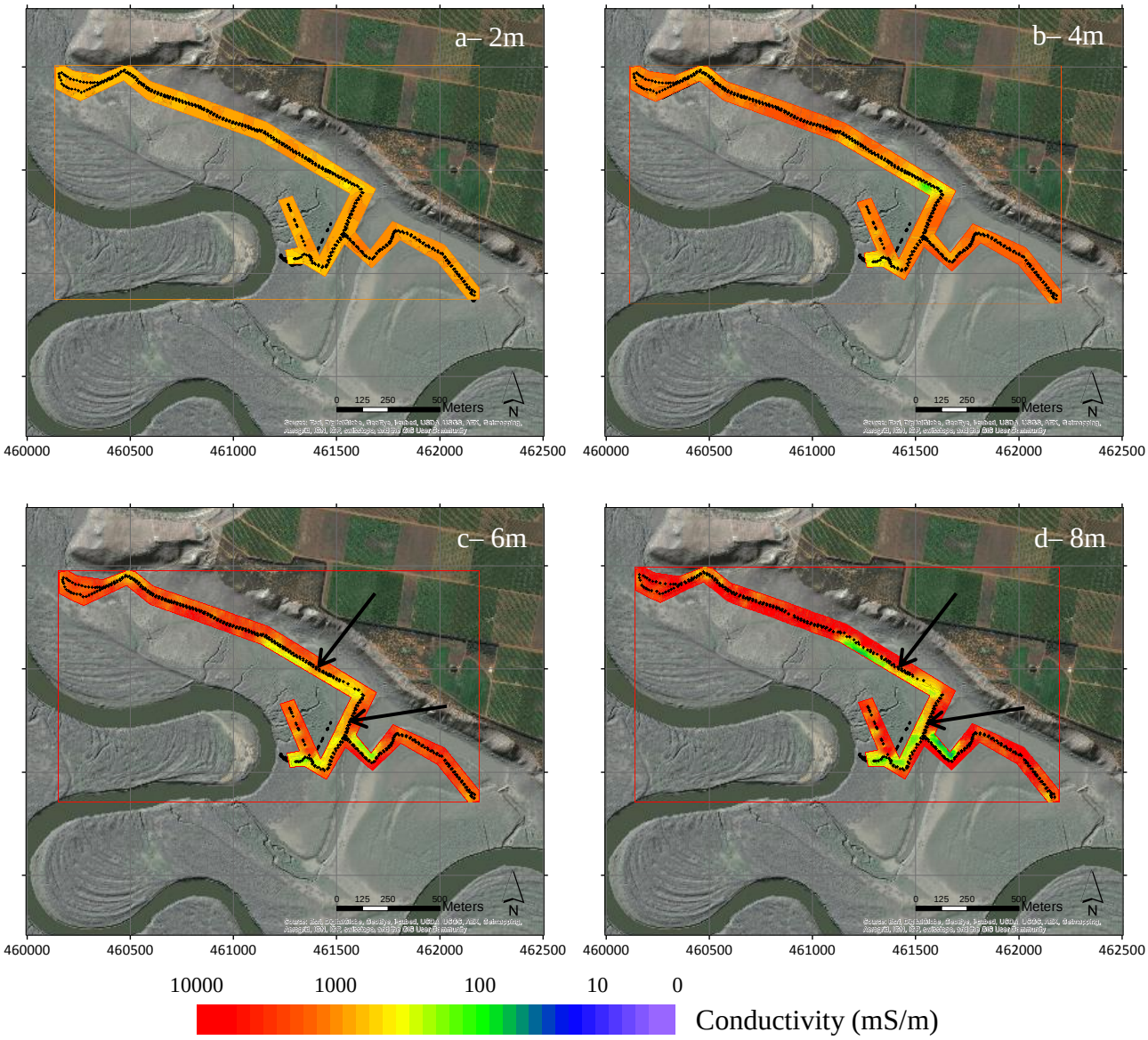

Figure 12: Inverted TEM depth models, a)-d) map views of the conductivity model for 2, 4, 6, and 8m. Data were collected in December 2011 using a single turn antenna configuration, nine months after the height of the 2010/2011 flood, to characterise the change in conductivity distribution. Survey locations are represented by black markers. Arrows indicate errors associated with the single-turn configuration. See Figure 4 for base-map information.

Single-turn towed TEM data from 2011 contain approximately 25000 data points that were inverted to produce 2D depth-sliced sub-surface models (Figure 11). There are problems with this data that can be seen in these plots. In two notable areas, indicated by arrows in Figure 12 where a section of track was surveyed twice, data are significantly different between the two runs. It is unknown what caused this, as it is not evident in the triple turn data.

Static TEM data from 2011 contain approximately 450 data points that were inverted to produce a 2D three layered sub-surface model (Figure 13). Despite termination of the LMPB, the freshwater lens is observed to retain a similar distribution post flooding, when compared to data collected in 2008. A small resistor has appeared at the western end of the line below 35m depth. Two distinct conductors have formed either side of the LMPB at 461355m and 461400m.

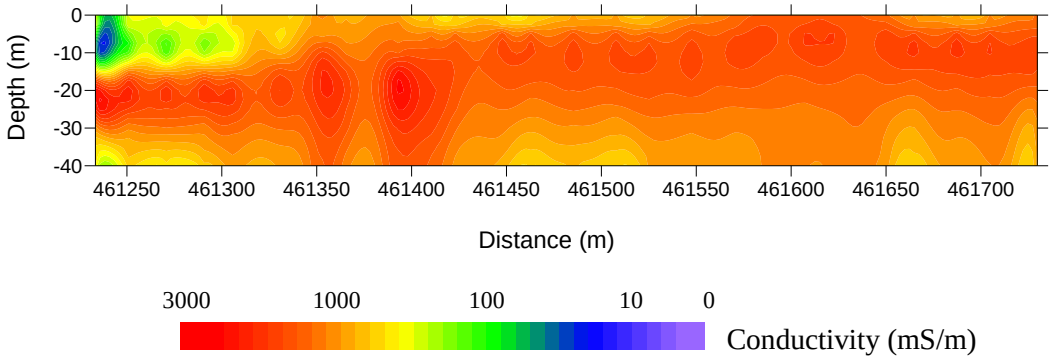

Figure 13: Static TEM vertical cross-section of inverted conductivity data collected in December 2011. The profile is given by transect B3 in Figure 4.

TEM SURVEY 2013

Three data sets were collected in July 2013, aiming at determining the conductivity distribution after river recession following overbank flows. Figure 14 shows the triple turn towed TEM, Figure 15 shows a single turn TEM trial and Figure 16 shows the static B3 transect. It is important to note that SIS and LM pumping recommenced in March and April 2003, respectively.

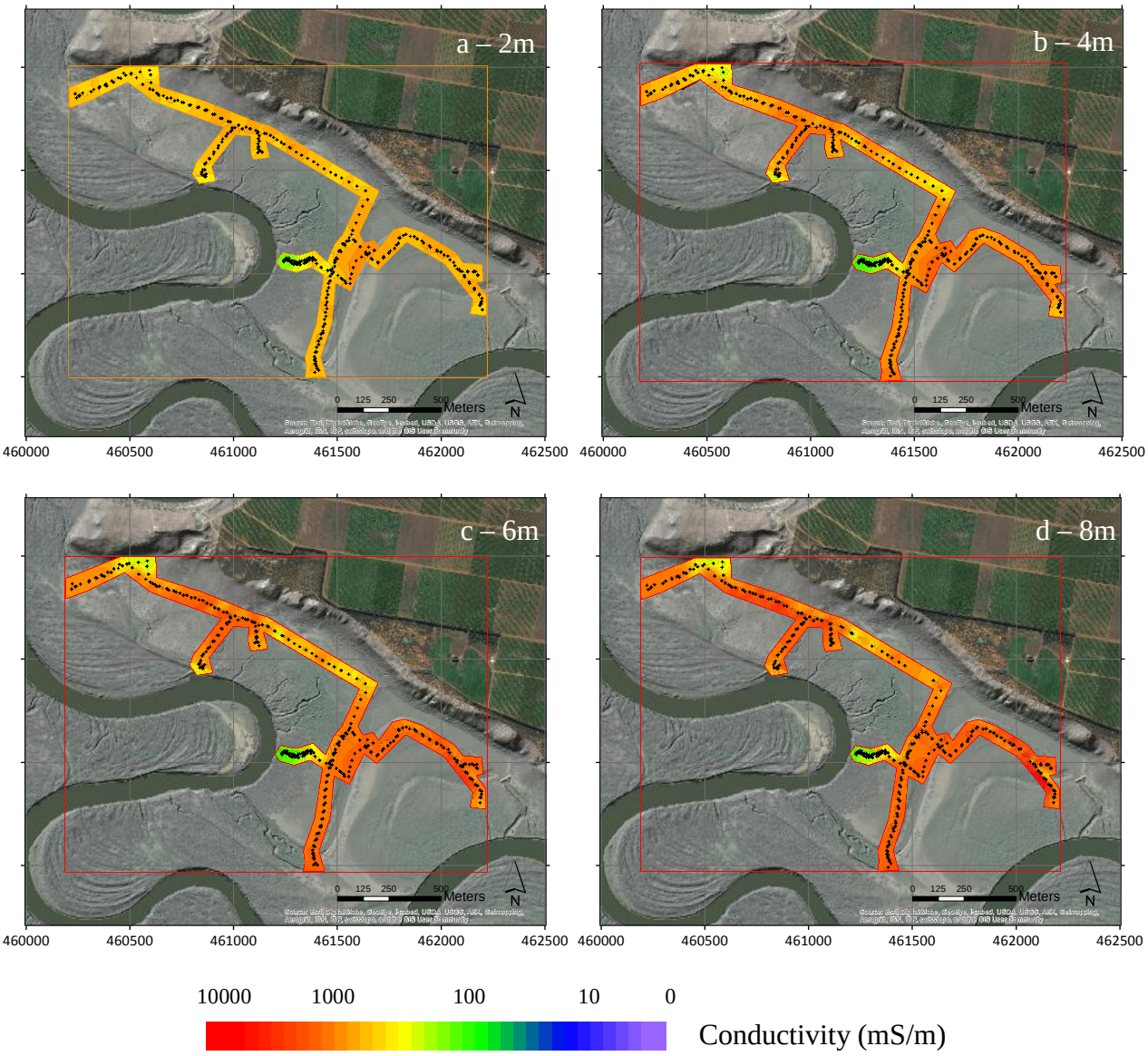

Figure 14: Inverted TEM depth models, a)-d) map views of the conductivity model for 2, 4, 6, and 8m. Data were collected in July 2013 using a triple turn antenna configuration, approximately two years the height of the 2010/2011 flood, to characterise the change in conductivity distribution. Survey locations are represented by black markers. See Figure 4 for base-map information.

Triple-turn towed TEM data from 2011 contain approximately 30000 data points that were inverted to produce 2D depth-sliced sub-surface models (Figure 14). Interpretation of Figure 14 suggests the floodplain is more resistive at all depths, particularly in the 6-8m range, signifying a decrease in the presence of salt in the near-surface alluvium and groundwater, compared to the 2011 data set (Figure 11). Similarly, the western resistor on B3 (see Figure 4) has migrated further east since 2011.

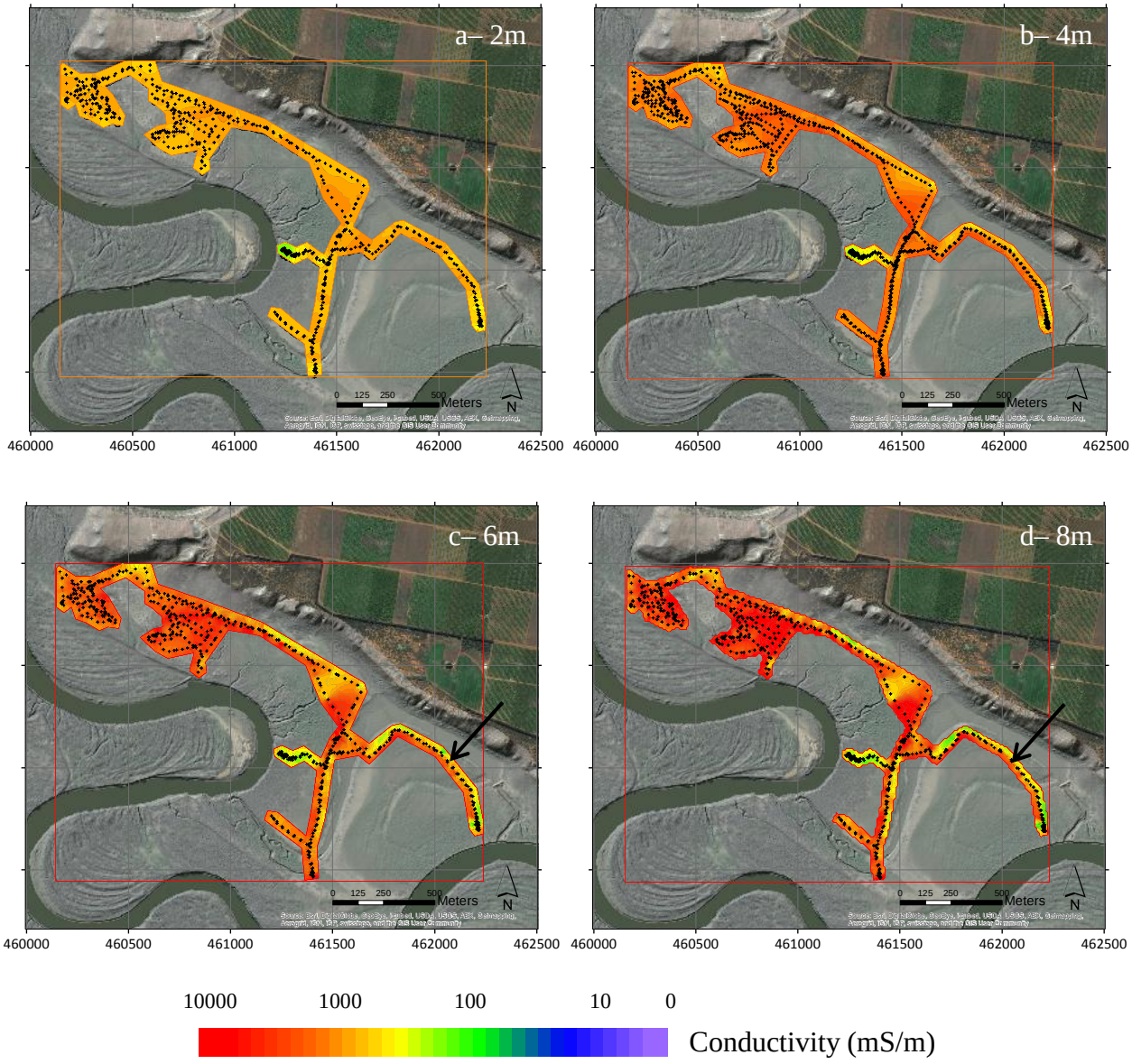

Figure 15: Inverted TEM depth models, a)-d) map views of the conductivity model for 2, 4, 6, and 8m. Data were collected in July 2013 using a single turn antenna configuration, approximately two years after the height of the 2010/2011 flood, to characterise the change in conductivity distribution. Survey locations are represented by black markers. Arrows indicate errors associated with the single turn configuration. See Figure 4 for base-map information.

Single-turn towed TEM data from 2011 contains approximately 30000 data points that were inverted to produce 2D depth-sliced sub-surface models (Figure 15). Single turn data from 2011 is similar to single turn data from 2013, as it had trouble repeating parts of the floodplain that have already been surveyed. Arrows show locations in this data set that did not repeat well. The cause of this is unknown, although it appears that the single turn configuration is more affected by local noise than triple turn.

Static TEM data from 2013 contains approximately 450 data points that were inverted to produce a 2D three layered sub-surface model (Figure 16). When compared with previous data sets, a reduction in floodplain conductivity is observed in all layers of the model, particularly at depth. The freshwater lens has increased, with its effects observed in excess of 100m from the river bank. The resistor below 30m at the western end of the line has increased horizontally by approximately 70m, mirroring the near surface freshwater lens. Conductors either side of the LMPB have reduced, and appear to have migrated west by 15-20m towards the river. In addition, two resistors have formed either side of the bore at approximately 461355m and 461440m. The rest of the line remains highly conductive, however conductivities above 1000mS/m have been limited to 20m depth, with distinct freshening occurring below this.

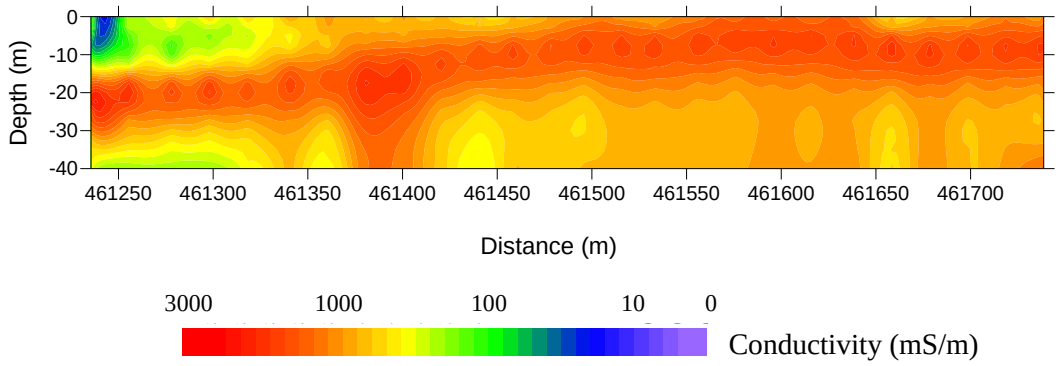

Figure 16: Static TEM vertical cross-section of inverted conductivity data collected in July 2013. The profile is given by transect B3 in Figure 4.

COMPARISONS

Analysis of the TEM results (Figure 6 – 16) indicates change in the observed conductivity distribution during fluctuating climatic conditions. Four methods used for TEM data collection performed with variable success. Static TEM using 20m x 20m antennas is a well-established method, and was therefore classed as the base to validate other TEM data sets. Static TEM successfully identified lateral and vertical change in the distribution of fresh and saline groundwater during Living Murray pumping, as well as change after overbank flows on the field site. Triple turn moving TEM correlated well with static data, while improving in horizontal resolution and acquisition rates. Both techniques were able to monitor bank recharge and associated freshwater flux, however triple turn data improved near surface resolution, aiding in the examination of soil salinity as indicated in Figure 17.

The decreased transmitter size used in the towed TEM method restricts imaging depth to approximately 10m, whereas static loops can image up to 80m, and therefore successfully quantify conductivity to well below the base of the Loxton Sands aquifer. Consequently, it was the only method that identified lateral flow of saline groundwater at depth. The associated freshening induced by base flow is shown in Figure 16, identified to be contained below 15-20 m, and likely occurred post river regression after flooding.

Moving TEM: Comparison of configurations

Three configurations were used during the surveys shown here. Most data were collected using the triple-turn method. Some data were collected using the single turn

method, and in 2008 data were collected using a triple-turn out-of-loop configuration. The out of loop configuration had difficulty in imaging discrete resistive zones, such as the freshwater lens at the western end of B3, interpretation of the data was therefore problematic.

Figure 17 shows depth sections along B3 that have been produced from single turn towed, triple turn towed and static TEM data from July 2013to identify correlation between the configurations.

In theory a single turn transmitter and receiver setup would produce superior results compared with triple turn TEM, as it reduces mutual inductance between antennas. To compensate for the decrease in antenna size, the gain or sensitivity on the receiver is increased. The 2011 single turn data (Figure 12) is similar to the 2013 single turn data (Figure 15) in the sense that it is on the whole slightly more conductive than triple turn data.

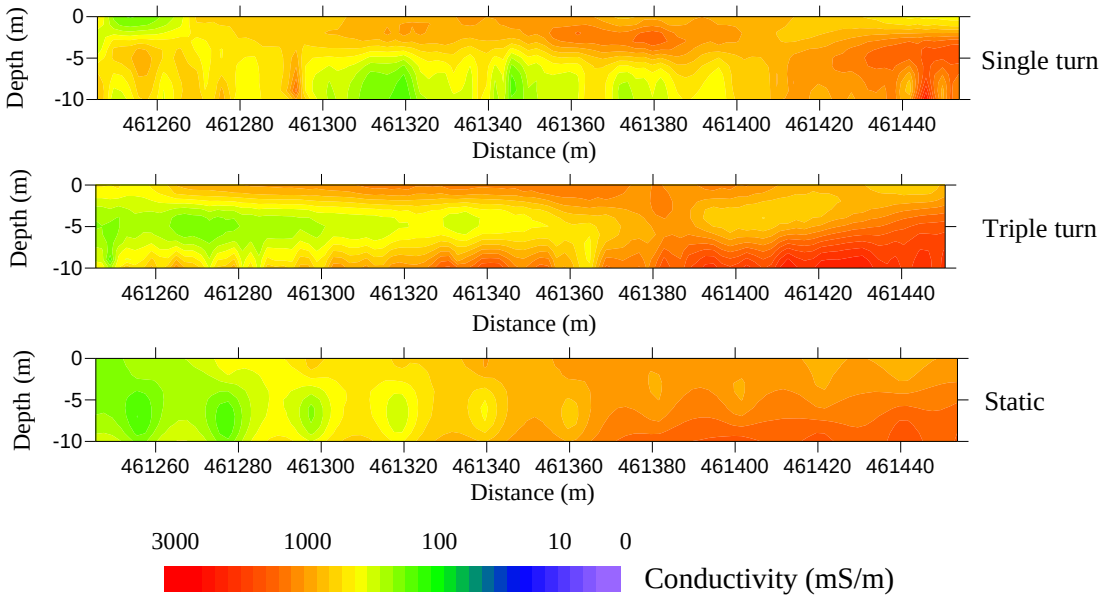

Figure 17: Single turn towed TEM and static TEM vertical cross-sections of inverted conductivity data. Acquired in July 2013 from the western limb of transect B3.

Despite the differences in surveying method, static, triple turn and single turn TEM data acquisition are based on the same principles and should correlate to a reasonable extent. Analysis of Figure 17 suggests that the triple turn configuration produces data that are more similar to the static data, than data collected using the single turn configuration. The zone east of 461400m displays some correlation with the profiles, i.e. becoming more conductive with depth, however discrete features are inconsistent. Triple turn towed TEM data correlates with static TEM data, indicating consistent repeatability between methods.

The primary concern with single turn data is poor repeatability in sections of depth slices, resulting in distinct conductivity divides along arbitrary transects, shown in Figures 12 and 15. Features observed in the data are highly unlikely, given the straight geometry observed, and change in conductivity on the scale of up to two orders of magnitude (1000mS/m decreasing to 100mS/m) over several meters.

Terrain Conductivity Meter Data

Two similar frequency domain electromagnetic (FEM) conductivity meters were used for this study. A Geonics EM31 was used to collect the pre flood data in 2006 and 2008. A GF Instruments CMD-4 was used to collect post flood data in 2013. Both systems give a bulk conductivity based on the top 2 – 6m of the subsurface. This measurement is typically a representation of the regolith and surface of the water table, regulated by their relative conductivity. It can be difficult to determine depth of investigation, as the instruments provide a single estimate of conductivity at a single frequency, therefore depth information cannot be constrained. In addition, like all EM techniques the data is

affected by a range of variables, including clay content, pore salinity and moisture content, as well as groundwater depth and salinity.

All data were LIN corrected, due to limitations associated with the LIN approximation that FDEM machines use to infer ground conductivity (Reid and Howlett 2001). High conductivities in the field area reduce skin depth close to the coil separation of the device, rendering the LIN assumption incorrect (Beamish 2011).

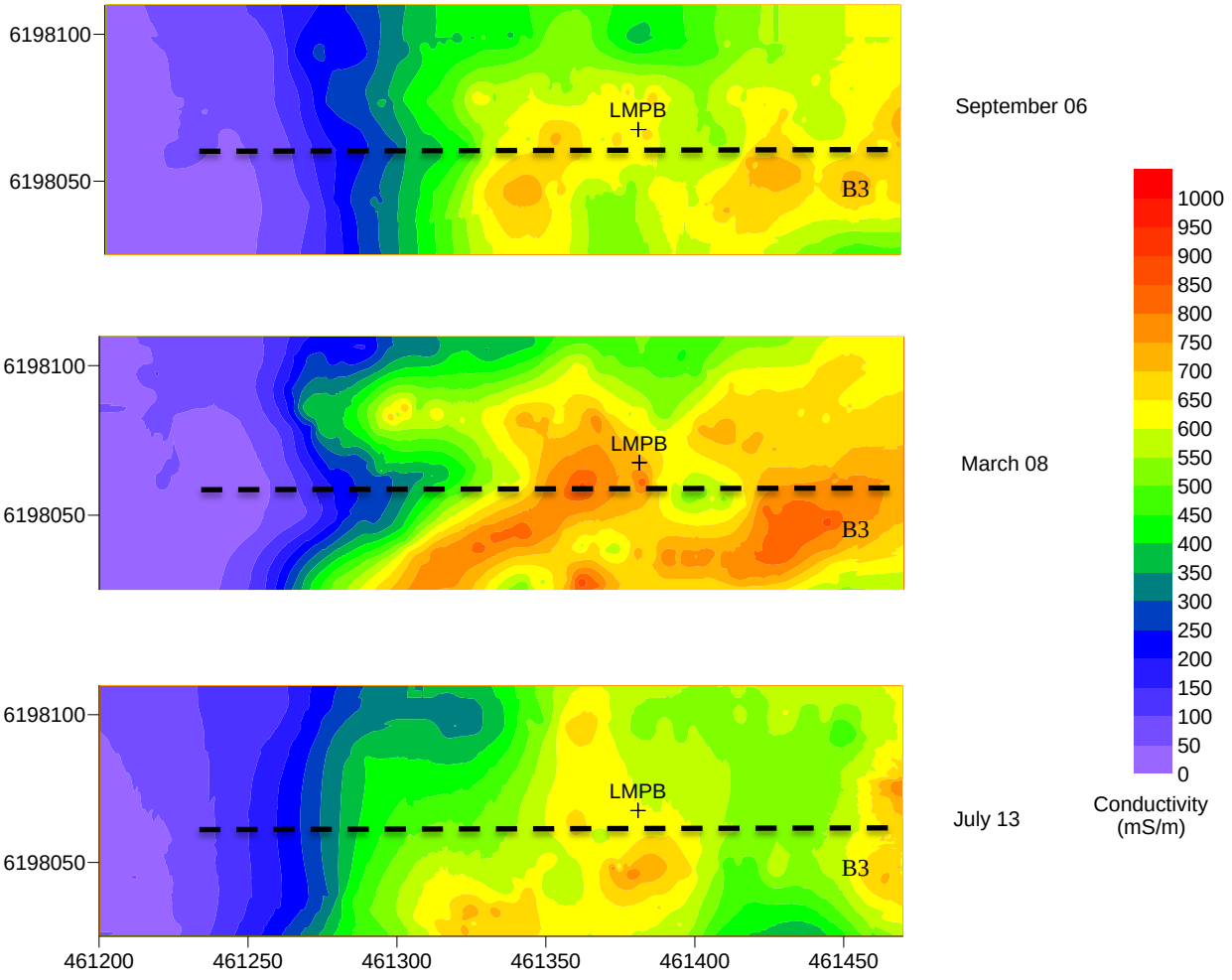

Figure 18: LIN corrected EM31 data from a zone within the field area (see Figure 4 for location). Data were collected during drought conditions, as well as after the 2010/2011 flood, to characterise the respective conductivity distribution within the first 2m – 6m.

Terrain conductivity data shown in Figure 18 contain approximately 1000 data points that were gridded using kriging to produce 2D conductivity maps. A distinct freshwater lens is evident on the western edge of all three contour maps, and appears to have shifted position between 2008 and 2013. In 2008, the effects of the LMPB are observed either side of line B3, whereas a recession in the lens occurred on the line itself. Despite an increase in the distribution of the freshwater zone, conductivity slightly increased, due to a reduction in induced bank recharge.

The distribution of strong conductors increased in 2008 within the central and eastern zones of the survey site, likely caused by increased evaporation and evapotranspiration consolidating salt at the height of the drought. Conductivities have doubled in some areas from 500mS/m to in excess of 1000mS/m. In 2013, the same area freshened after natural flooding, with conductivities retreating to a similar range as seen in 2006. The highly conductive zone, surrounding the LMPB pre-flooding reduced by a factor of 2 in some areas.

Groundwater Conductivity Data

Groundwater conductivity was monitored from January 2006 to July 2013, initially to determine the effectiveness of the LMPB and Salt interception Scheme (SIS). A YSI XLM600 multi-parameter groundwater sonde was used to examine the interface between the highly saline groundwater and the overlying low salinity lens induced through pumping. Bores were monitored after LMPB and SIS bores were turned off, due to floodplain inundation following 2010/2011 flooding. Despite pumping being re-established in 2013, it is thought that most of the change in the distribution of conductivity (salinity) observed after the flood is in response to floodplain inundation.

Groundwater sonde data were quality controlled by removing outliers and 2D vertical cross-sections were gridded by kriging (Figure 19). 16 groundwater profiles along line B3 (see Figure 4) were produced. Acquisition commenced 6 months prior to initial Living Murray (LM) pumping and 6 months after commencement of the floodplain SIS. Interpretation of January 2006 sonde data indicates natural bank recharge on the floodplain extending to a distinct halocline at approximately 2.5m depth. The freshwater lens was limited laterally, with saline groundwater in excess of 5000mS/m evident from the top of the water table. Profiles from the commencement of LM pumping (August 2006) to the 2010/2011 flood when pumping stopped (November 2010) project the effectiveness of the LM pumping trial, as has been reported on by Berens, (2009). For the purpose of this study, the distribution of both the freshwater lens and saline groundwater are of interest post-flooding.

Despite recommissioning of the SIS and LMPB in March and April 2013 respectively, it is unlikely that they would have had much effect on any change to the distribution of groundwater, because of the short operation time. The LMPB recommenced in April 2013 and was operational for approximately 3 months before the 2013 data sets, shown previously, were collected. The effect of the LMPB within a similar timeframe is evident in the period when the bore was first commissioned, from August – October 2006 (Figure 19).

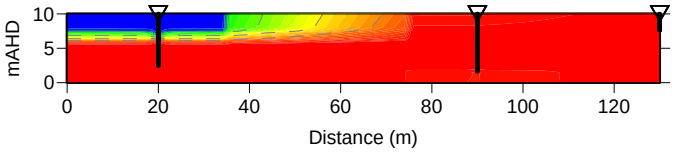

January 06

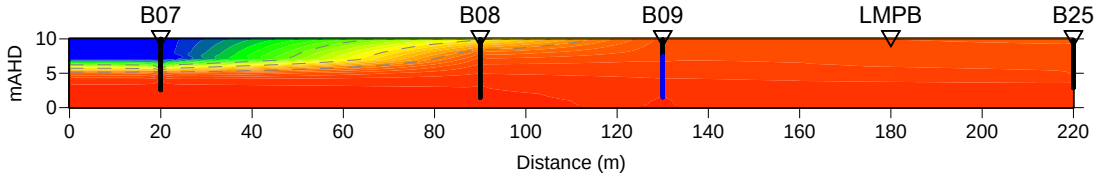

July 06

Commencement of LM pumping (August 2006)

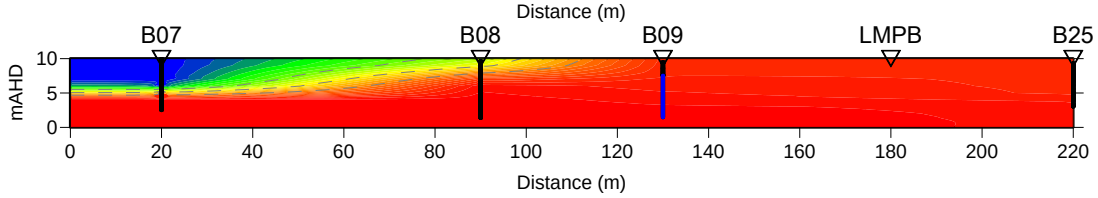

August 06

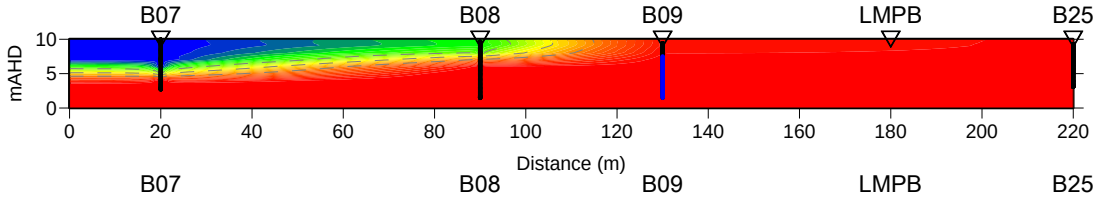

October 06

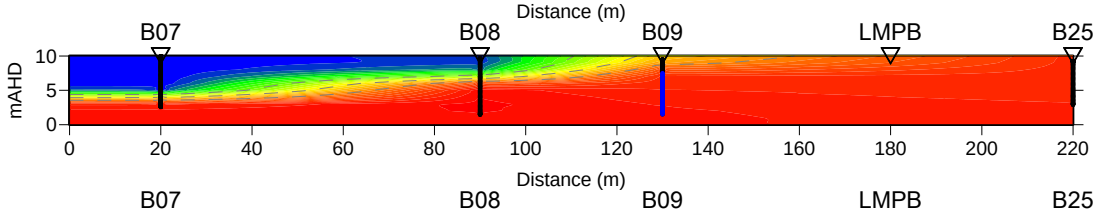

November 06

Stop to SIS & LM pumping (November 2006)

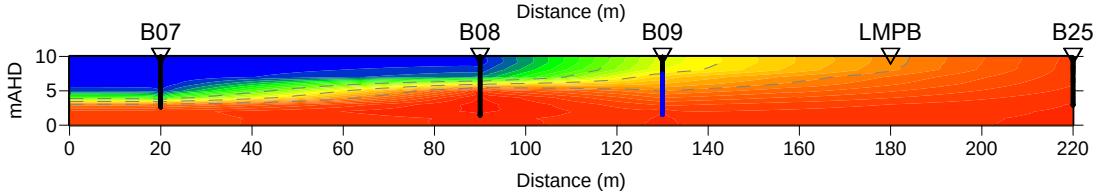

December 06

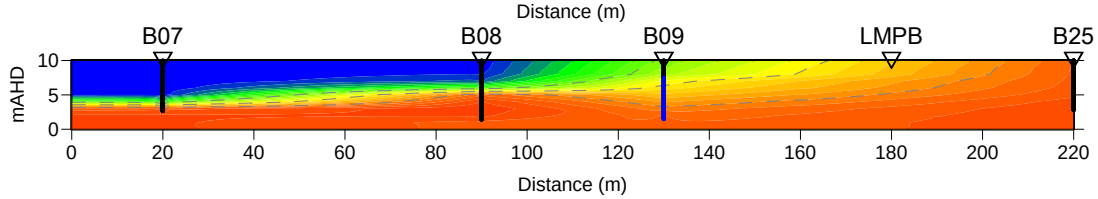

January 07

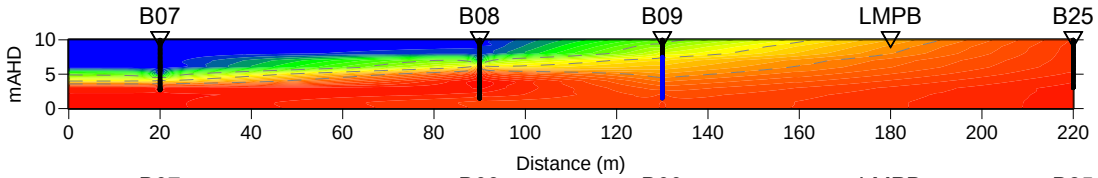

March 07

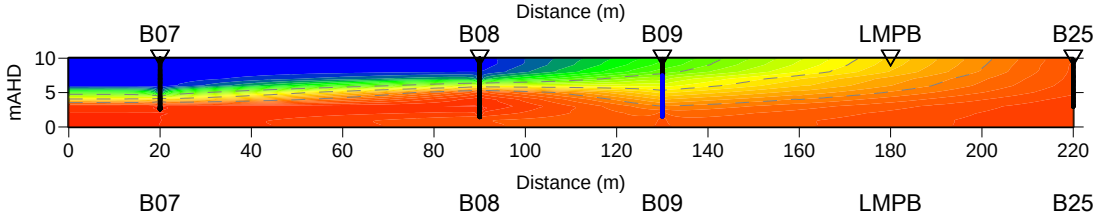

April 07

Recommencement of SIS & LM pumping (May 2007)

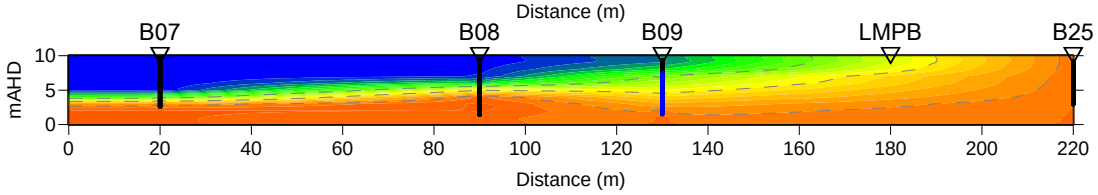

July 07

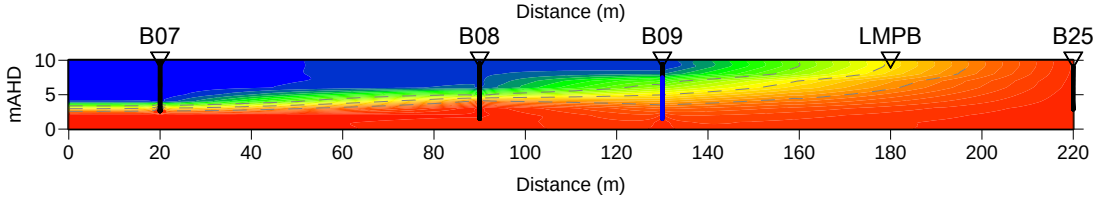

October 07

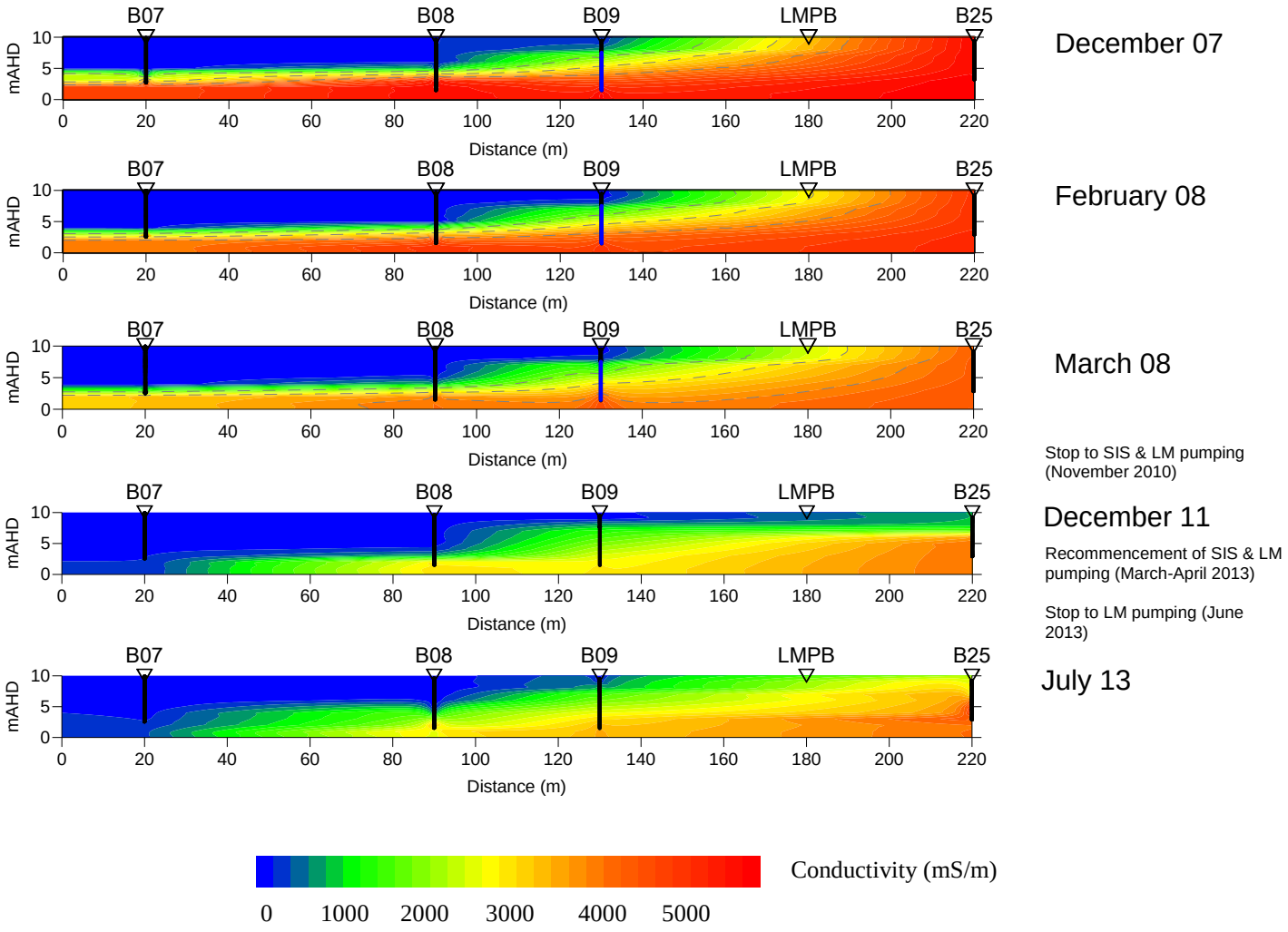

Figure 19: Downhole sonde profile of transect B3 from 4 observation bores. They indicate the development of the freshwater lens and underlying saline groundwater.

Prior to December 2011, LM pumping stopped for 18 months, as the floodplain experienced overbank flows. Freshening observed in December 2011 was therefore directly related to floodplain inundation. Data from December 2011 identified freshening at bore B07, with the entire profiles salinity below 200mS/m. Bore B08 recorded conductivities in excess of 200mS/m below 7m depth, an increase of 2 m since flooding. The near-surface was unaffected at B09, however saline groundwater became more resistive towards the bottom of the profile falling from over 3000mS/m to 1000-2000mS/m range. Bore B25, at the eastern end of the transect experienced freshening for the first time since groundwater profiling. The top of the profile reduced in

conductivity from 5000mS/m to 2000mS/m. Bore B25 was installed as a control observation bore inland of the LMPB. Salinity changes here are mostly independent of pumping, suggesting salt mobilisation through floodplain inundation.

Over 2 years after the peak of the flood, the July 2013 data acquired indicates a slight recession in the lateral extent of the freshwater lens previously evident at bore B25. However, bore B07 remained fresh to the base of the profile, and only a small rise in the height of the saline groundwater body was observed at bored B08 and B09. Despite upwards dispersion of salt observed at B25, salinity capped at 4000mS/m, a reduction of over 1000mS/m from December 2011. This supports a lateral or vertical mobilisation of saline groundwater from depth, as opposed to the near surface.

DISCUSSION

Analysis of floodplain subsurface conductivity distribution identified groundwater freshening on the field site, in response to flooding. Groundwater freshening through vertical infiltration and bank recharge, as these are both relatively shallow processes, should be observable in the groundwater sonde data, as well as in the shallowed part of the TEM data sets and the terrain conductivity data. However, groundwater freshening through lateral flow is not a process that has been observed in the lower reaches of the River Murray, as this is a deeper process that is difficult to observe. As expected, lateral flow was not detected until over two years after the flood, following recession of the river, and is seen mostly as freshening in the deeper parts of the static TEM data sets.

Static and towed TEM collectively identified all three floodplain freshening mechanisms, as it produced high resolution data in the near-surface and at depth.

Vertical infiltration of flood waters through the unsaturated zone resulted in a reduction in soil salinity. TEM profiles indicated a slight reduction in conductivity in the unsaturated zone, however not as much as expected when Holland et al. (2013) is examined. Holland et al. (2013) suggested a 40% reduction in soil chloride on Clark's floodplain, facilitated by upwards migration of low-salinity groundwater. Salinity of the vadose zone is difficult to detect with EM methods, due to the increased number of variables that exist within the zone, notably the concentration of clay and seasonal fluctuation of moisture. Despite this, it is thought the increase in resistivity within the top 4m of the floodplain can be attributed to a reduction in soil chloride facilitated by vertical infiltration of flood water.

In addition, upwards movement of low-salinity water through the capillary zone post flooding would also facilitate a reduction in soil chloride concentration. This was interpreted in the 2013 TEM data in areas close to the river that increased in resistivity from 2011, where the Coonambidgal Clay is sparse and saturation of near-surface resistive sediments would not increase conductivity.

TEM data were able to identify change in the distribution of the freshwater lens throughout the entire data chronology. Once again, monitoring below the conductive Coonambidgal Clay can be problematic, as it only exists as a thin alluvial layer above most of the recharge zone (Lewis et al. 2008). The full extent of bank recharge was hard to identify further from the river, as clay thickened.

The original hypothesis of this study was to test the ability of overbank flows to reduce groundwater salinity through lateral flow of groundwater following river withdrawal. It

was assumed that flow from a losing floodplain would be facilitated near the top of the water table, where the highest hydraulic gradient exists. Inverting the static TEM data allowed observation of both the Monoman and underlying Loxton aquifers, as seen in Figures 6, 8, 10, 13 and 16. These data supported the initial hypothesis, suggesting a lateral movement of saline floodplain water at depth through base flow.

The first observation of flow from the floodplain to the river occurred in December 2011, identified by freshening below 35 m depth (Figure 13). It appears that groundwater at depth is flushed out of the system, as infiltration from the surface and the river bank occurs, increasing aquifer pressure. Between December 2011 and July 2013 base flow increased, likely occurring within the past year when the river level rapidly retreated (identified in Figure 5). High salinity groundwater has been given preference by the base flow mechanism, as it appears to be the only groundwater zone to decrease in the system. This is related to increased transmissivity within that layer of alluvium, or the relative density of the saline body.

From 2011 to 2013, the zone below 20m east of the LMPB greatly reduced in conductivity, likely due to an accession of salt (Figure 16). Similarly, the conductive band above 20m has been consolidated, potentially acting as a groundwater pathway further facilitating lateral flow. As groundwater ascended, less-saline regional groundwater entered the floodplain, flowing from the adjoining Loxton Sands aquifer in the adjacent highland.

Two vertically extensive conductors visible in the 2011 TEM data at 461350m and 461380m (Figure 13), likely associated with the LMPB. The first conductor (from the

west) migrated approximately 10m west from 2011 to 2013, further supporting the likelihood that lateral flow was active within the conductive seam. The larger conductor shares the same location as the LMPB, likely caused by a leak or salt accumulation associated with pumping, as it's the only zone along the entire profile that noticeable increased since 2005. It did become more resistive from 2011 to 2013, relating to an inflow of lower salinity regional groundwater from the Loxton Sands.

Vertical infiltration of flood water is relatively hard to identify with EM techniques on the lower Murray floodplains, as the top most alluvial unit is a conductive clay. Shallow terrain conductivity data produced high resolution lateral results relating to the near-surface conductivity, representing soil salinity and the upper water table. The issue with FEM techniques, is the uncertainty of which conductor is being imaged. White et al. (2009) and Telfer et al. (2012) suggest terrain conductivity data are indicative of groundwater conductivity, as the watertable depth is at most a few meters. However, water table depth measurements recorded in July 2013 indicate an average depth of 3.5m; this may suggest conductivity measured with FEM systems reflects vadose zone salinity, rather than groundwater salinity.

The nature of the Coonambidgal Clay causes it to thin towards the river (Lewis et al. 2008), reducing its influence on sub-surface conductivity measurements in this zone. Consequently, terrain conductivity data on the western side of the acquisition area (Figure 4) are assumed to represent the distribution of the freshwater lens. As clay thickens away from the river, conductivity is assumed to represent soil chloride concentration, east of 461300m, shown in Figure 18. This zone increased in resistivity

from 2008 to 2013, driven by dissolution of soil chloride during vertical infiltration of flood water.

An accurate representation of the distribution of the freshwater lens driven by bank recharge was deduced from groundwater sonde data. Natural bank recharge is difficult to monitor near transect B3 on Clark's Floodplain, due to the influence of the Living Murray Pumping Bore (LMPB). Bank recharge was induced while the bore was operational, however this only took place from early April to Early June 2013, not dramatically affecting our results. The inflow of low salinity river water into the floodplain groundwater system produces a freshwater lens at the surface, which is important for tree-water availability (Doody et al. 2009, Holland et al. 2009). In 2008, the induced freshwater lens extended 130m from the river bank, as indicated by bore B09, and there was some response at bore B25 as well in December 2011 (figure 18). This suggests an increase in the distribution of the freshwater lens through either bank recharge or vertical infiltration of low-salinity water by up to 90m. Bore B25 was originally installed as a control, i.e. far enough inland that it would be unaffected by the effects of LM pumping.

Collectively, the three conductivity data acquisition methods were able to identify three floodplain groundwater freshening mechanisms. Shallow TEM and terrain conductivity data were both able to identify vertical infiltration of flood water, interpreted by a decrease in conductivity in the vadose zone. Both methods also identified fluctuation in the distribution of the freshwater lens and associated natural and induced bank recharge. Groundwater sonde data (Figure 19) were able to quantify the full extent of freshening

through bank recharge and vertical infiltration by identifying the distinct halocline that exists between the fresh and saline groundwater. Despite all three techniques identifying an increase in the distribution of the freshwater lens in 2013, conductivities were slightly elevated compared to past observations. This is likely due to the system freshening under natural bank recharge, as opposed to induced recharge. It is also important to note that the water table and river level were close to equilibrium as of July 2013 (approximately 10.5 m) and potentially earlier, meaning natural bank recharge may have stopped before July. Salt would have concentrated during this period through evapotranspiration and evaporation, increasing conductivity.

Static TEM was the most successful survey method, as it produced high resolution data in the near surface, as well as at depth. Towed TEM is also an efficient survey method with broad lateral resolution, and therefore accurately identifies the horizontal extent of freshening. However, the towed system is limited to shallow soundings, and in some cases is not sufficient in identifying lateral flow. It is also important to note that the out of loop system trialled in 2008 did not adequately constrain conductivity within resistive regions. Similarly, single turn data acquisition trialled in 2011 and 2013 are inconsistent with the well-established static TEM method, rendering its data less interpretable. The triple turn TEM method provided the most useful out of the towed configurations. If surveying is to be continued on Clark's floodplain it is suggested that this method, along with the static TEM method be utilised.

Through analysis of the above geophysical data, the importance of flooding on reducing floodplain salinity has been reinforced. Lateral flow of highly saline water at depth was identified as a key feature of groundwater freshening following floodplain inundation. It

is unlikely that this mechanism will progress until another major flooding event occurs, due to the river and water table being in equilibrium at present.

It is worth considering whether that freshening through lateral flow of saline groundwater was primarily driven by the Bookpurnong SIS. This was operating for a period of approximately four months prior to the 2013 survey. The effect of this scheme is assumed to have little effect on the system in this study, given its short operation time prior to data acquisition. However the true influence of the SIS is unknown, and further work could be conducted in the following year to analyse the change in the floodplains sub-surface conductivity independent of natural inundation freshening mechanisms.

CONCLUSIONS

Floodplain groundwater freshening through lateral flow of saline groundwater after a natural inundation event was a previously unidentified mechanism. The primary focus of the Clark's Floodplain survey was to map conductivity in the alluvial sediments existing on and below the floodplain. The analysis of historical and current geophysical data sets has provided an insight into the changing distribution of conductivity within the floodplain system during a range of climatic conditions. The three geophysical techniques utilised, collectively provided conductivity data that was interpreted to identified a reduction in floodplain salinity at the near-surface and at depth. TEM proved to be the most valuable acquisition method, as data was used to classify all three freshening mechanism after overbank flows.

A reduction in soil chloride was identified post flooding, assumed to be driven by vertical infiltration of low salinity flood waters. In addition, the extent of bank recharge was also monitored at the near surface, enabled through the observation of a resistive

lens at the river end of the survey transect. Finally, highly saline groundwater was expelled from the system at depth through lateral flushing, following river recession. It was identified by an increase in resistivity from historic data to 2013 data. Further research could be undertaken to better understand the duration of deep base flow, as well as determining the relative influence SIS pumping may have on the mechanism. Natural inundation and associated lateral flow of saline groundwater is a major freshening mechanism within floodplain systems, particularly within the Murray Basin.

ACKNOWLEDGMENTS

This study was initiated by Michael Hatch who provided background knowledge of past geophysical surveying, as well as organising fieldwork for this study and providing constant support. I also acknowledge the support of Volmer Berens, who provided historical data regarding the field site and use of a groundwater profiler. I would also like to thank Peter Forward for providing access to Clark's Floodplain and information regarding the salt interception schemes in the region. In addition, I acknowledge GRS for use of their NanoTEM system, CSIRO for use of their CMD-4 and Thomas Fotheringham for his assistance with fieldwork.

REFERENCES

ACWORTH R. L. & JANKOWSKI J. 2001 Salt source for dryland salinity - evidence from an upland catchment on the Southern Tablelands of New South Wales, *Soil Research,* vol. 39, no. 1, pp. 39-59.

BEAMISH D. 2011 Low induction number, ground conductivity meters: a correction procedure, *Applied Geophysics,* vol. 75, pp. 244-253.

BERENS V., WHITE M. & SOUTER N. 2009a Bookpurnong Living Murra Pilot Project: A trial of three floodplain water management techniques to improve vegetation. Adelaide, SA: Government of South Australia, through Department of Water, Land and Biodiversity Conservation.

BERENS V., WHITE M. & SOUTER N. 2009b Bookpurnong Living Murray Pilot Project: Injection of river water into the floodplain aquifer to improve vegetation condition. Adelaide, SA: Government of South Australia, through Department of Water, Land and Biodiversity Conservation.

BREN L. J. 1992 Tree invasion of an intermittent wetland in relation to changes in the flooding frequency of the River Murray, Australia, *Australian Journal of Ecology,* vol. 17, no. 4, pp. 395-408.

BROWN C. & STEPHENSON A. E. 1991 Geology of the Murray Basin, Southeastern Australia, *Bureau of Mineral Resources, Australia,* pp. 235-430.

BROWN C. C. 1989 Structural and stratigraphic framework of groundwater occurrence and surface discharge in the Murray Basin, southeastern Australia, *BMR Journal of Australian Geology & Geophysics,* vol. 11, pp. 127-146.

CARTWRIGHT I., *et al.* 2004 Hydrogeochemical and isotopic constraints on the origins of dryland salinity, Murray Basin, Victoria, Australia, *Applied Geochemistry,* vol. 19, no. 8, pp. 1233-1254.

DAHLHAUS P. G., *et al.* 2000 Salinity on the southeastern Dundas Tableland, Victoria, *Australian Journal of Earth Sciences,* vol. 47, no. 1, pp. 3-11.

DOODY T. M., *et al.* 2009 Effect of groundwater freshening on riparian vegetation water balance, *Hydrological Processes,* vol. 23, pp. 3485-3499.

FETTER C. W. 2001 Applied hydrogeology. Prentice Hall, Upper Saddle River, New Jersey.

FITTERMAN D. V. & STEWART M. T. 1986 Transient Electromagnetic Sounding for Groundwater, *Geophysics,* vol. 51, pp. 995-1005.

FORWARD P. D. 2004 South Australia's River murray salt interception scheme - history, performance and future directions. 1st National Salinity Engineering Conference Perth, Western Australia.

HATCH M., MUNDAY T. & HEINSON G. 2010 A comparative study of in-river geophysical techniques to define variations in riverbed salt load and aid managing river salinization, *Society of Economic Geologists,* vol. 75, no. 4.

HOLLAND K. L., *et al.* 2009 Effectiveness of artificial watering of a semi-arid saline wetland for managing riparian vegetation health, *Hydrological Processes,* vol. 23, pp. 3474-3484.

HOLLAND K. L., *et al.* 2013 Floodplain response and recovery: comparison between natural and artificial floods. Goyder Institute for Water Research Technical Report Series. Adelaide, South Australia.

JOLLY I. D., MEEWAN K. L. & HOLLAND K. L. 2008 A review of groundwater-surface water interactions in arid/semi-arid wetlands and the consequences of salinity for wetland ecology, *Ecohydrology,* no. 1, pp. 43-58.

JOLLY I. D., *et al.* 1998 The impact of flooding on modelling salt transport processes to streams, *Environmental Modelling & Software,* no. 13, pp. 87-104.

JOLLY I. D., WALKER G. R. & THORNBURN P. J. 1993 Salt accumilation in semi-arid floodplain soils with implications for forest health, *Hydrology,* no. 150, pp. 589-614.

LAMONTAGNE S., LEANEY F. W. & HERCZEG A. L. 2005 Groundwater–surface water interactions in a large semi-arid floodplain: implications for salinity management, *Hydrological Processes,* vol. 19, no. 16, pp. 3063-3080.

LEWIS S. J., *et al.* 2008 Assessment of Groundwater Resources in the Broken Hill Region. In DEPARTMENT OF RESOURCES E. A. T. ed. Canberra, ACT: Geoscience Australia.

MCNEILL J. D. 1980a Electromagnetic terrain conductivity measuremen at low induction numbers, *Geonics Limited Technical Note,* vol. 6.

MUNDAY T., *et al.* 2007 Frequency and/or Time Domain HEM Systems for Defining Floodplain Processes Linked to the Salinisation along the Murray River?, *ASEG - Perth, Western Australia*.

MUNDAY T., *et al.* 2005 Combining Geology and Geophysics to Develop a Hydrogeologic Framework for Salt Interception in the Loxton Sands Aquifer, Central Murray Basin, Australia *Australian Journal of Water Resources,* vol. 9, no. 2, pp. 163-168.

REID J., FITZPATRICK A. & GODBER K. 2010 An overview of the SkyTEM airborne EM system with Australian examples, *Preview* vol. 145, no. 26-37.

REID J. E. & HOWLETT A. 2001 Application of the EM-31 terrain conductivity meter in highly-conductive regimes, *Exploration Geophysics*, vol. 32, pp. 219-224.

REM-AQUATERAM. 2005 Salt Interception Scheme Concept Design Murtho and Pike River, Hydrogeology and Proposed Groundwater Modelling Approach. Department of Water, Land and Biodiversity Conservation.

ROLLS J. 2007 Berri, Loxton, and Renmark Irrigation Areas CDS Water: Implications of Flow and Quality Data. In GOVERNMENT OF SOUTH AUSTRALIA T. D. O. E., WATER AND NATURAL RESOURCES ed. Adelaide, SA.

SUMMERELL G. K., *et al.* 2000 Modelling current parna distribution in a local area, *Soil Research,* vol. 38, no. 4, pp. 867-878.

TAN K. P., *et al.* 2007 Determining the suitability of in-stream NanoTEM for delineating zones of salt accession to the River Murray: A review of survey results from loxton, South Australia.

TELFER A., *et al.* 2005 Instream NanoTEM: Providing increased resolution to stream salinisation and floodplain processes along the River Murray, southeast Australia, *Australian Journal of Water Resources*, vol. 9, pp. 155-161.

TELFER A., *et al.* 2012 River Murray floodplain salt mobilisation and salinity exceedances at Morgan, *Murray Darling Basin Authority*.

TELFER A. L., *et al.* 2004a Instream NanoTEM survey of the River Murray 2004: Blanchetown to Mallee Cliffs. AWE: Murray River Darling Basin Commission and Mallee Catchment Management Authority.

TELFER A. L., *et al.* 2004b Atlas of instream NanoTEM 2004: Blanchetown to Mallee Cliffs. pp. 30. Adelaide, SA: Murray River Darling Basin Commission and Mallee Catchment Management Authority.

WHITE M., BERENS V. & SOUTER N. 2009 Bookpurnong Living Murray Pilot Project: Artificial inundation of *Eucalyptus camaldulensis* on a floodplain to improve vegetation condition. Adelaide, SA: Department of Water, Land and Biodiversity Conservation.

APPENDIX A: BOOKPURNONG WATERING SITE – BASELINE DATA

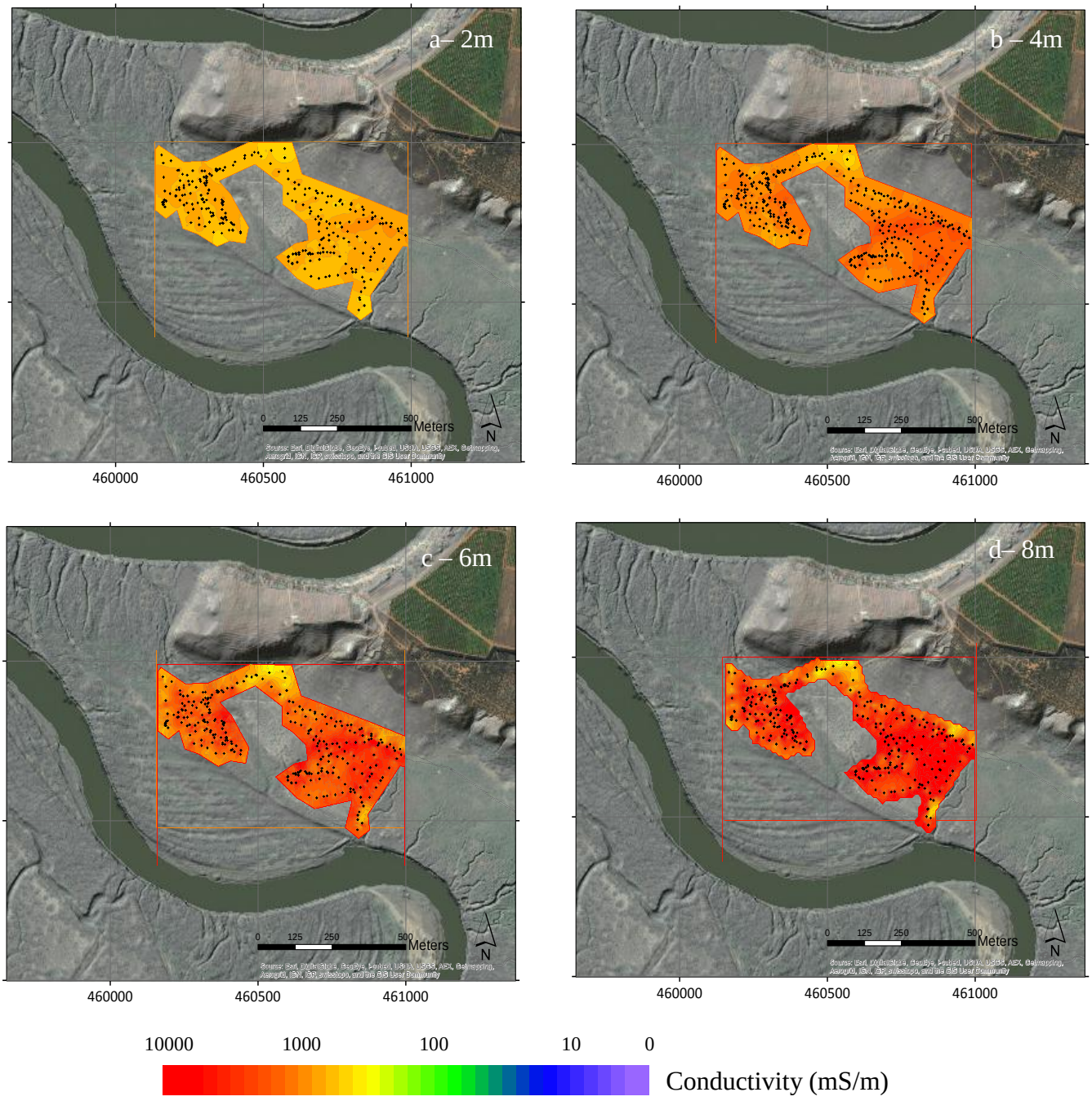

Figure 20: Inverted TEM depth slices at a - 2m, b - 4m, c - 6m and d - 8m depth overlayed on an air photo image and LiDAR elevation model of the field area. Data were collected in July 2013 after the 2010/2011 flood, to characterise the conductivity distribution.

The above baseline data was collected in an area that's in closer proximity to the irrigation district on the adjacent highlands. Consequently it is highly conductive at all

measured depths, ranging from approximately 1000 mS/m at 2m depth to over 10000 mS/m from 6m.